Mechanisms of Actin Rearrangements Mediating Platelet Activation

John H. Hartwig

Experimental Medicine Division, Brigham and Women's Hospital, and Departments of Medicine and Anatomy and Cellular Biology, Harvard Medical School, Boston, Massachusetts 02115

Abstract. The detergent-insoluble cytoskeleton of the resting human blood platelet contains ~2,000 actin filaments ~1 μm in length crosslinked at high angles by actin-binding protein and which bind to a spectrin-rich submembrane lamina (Fox, J., J. Boyles, M. Berndt, P. Steffen, and L. Anderson. 1988. *J. Cell Biol.* 106:1525–1538; Hartwig, J., and M. DeSisto. 1991. *J. Cell Biol.* 112:407–425). Activation of the platelets by contact with glass results within 30 s in a doubling of the polymerized actin content of the cytoskeleton and the appearance of two distinct new actin structures: bundles of long filaments within filopodia that end at the filopodial tips (filopodial bundles) and a circumferential zone of orthogonally arrayed short filaments within lamellipodia (lamellipodial network). Neither of these structures appears in cells exposed to glass with cytochalasin B present; instead the cytoskeletons have numerous 0.1–0.3-μm-long actin filament fragments attached to the membrane lamina. With the same time course as the glass-induced morphological changes, cytochalasin-sensitive actin nucleating activity, initially low in cytoskeletons of resting platelets, increases 10-fold in cytoskeletons of thrombin-activated platelets. This activity decays with a time course consistent with depolymerization of 0.1–0.3-μm-long actin filaments, and phalloidin inhibits this decay. Cytochalasin-insensitive and calcium-dependent nucleation activity also increases markedly in platelet extracts after thrombin activation of the cells. Prevention of the rise in cytosolic Ca^{2+} normally associated with platelet activation with the permeant Ca^{2+} chelator, Quin-2, inhibits formation of lamellipodial networks but not filopodial bundles after glass contact and reduces the cytochalasin B–sensitive nucleation activity by 60% after thrombin treatment. The filopodial bundles, however, are abnormal in that they do not end at the filopodial tips but form loops and return to the cell body. Addition of calcium to chelated cells restores lamellipodial networks, and calcium plus A23187 results in cytoskeletons with highly fragmented actin filaments within seconds. Immunogold labeling with antibodies against gelsolin reveals gelsolin molecules at the ends of filaments attached to the submembrane lamina of resting cytoskeletons and at the ends of some filaments in the lamellipodial networks and filopodial bundles of activated cytoskeletons. Addition of monomeric actin to myosin subfragment 1–labeled activated cytoskeletons leads to new (undecorated) filament growth off the ends of filaments in the filopodial bundles and the lamellipodial network. The simplest explanation for these findings is that gelsolin caps the barbed ends of the filaments in the resting platelet. Uncapping some of these filaments after activation leads to filopodial bundles. The calcium transient associated with platelet activation induces fragmentation of peripheral actin filaments by free gelsolin, and the resulting actin fragments, after dissociation of gelsolin from the filament ends, nucleate barbed-end growth of the lamellipodial network.

THE human blood platelet exemplifies the importance of actin and actin-associating proteins in cell motility. Actin represents about a fifth of the total protein in platelets which circulate as flat oval discs that upon stimulation with a variety of agents including ADP, thrombin, collagen, and glass transform into compact spheres from which extend spines (filopodia) and veils. Actin assembly onto the fast growing ends of actin filaments (the barbed ends of myosin head fragment-decorated filaments) accompanies these shape changes. The evidence for this assertion is that actin filament bundles with their barbed ends oriented outward are the major structures within the filopodia formed during platelet activation, the fraction of intracellular actin that is polymeric rises as the platelets change shape, and cytochalasins, which block addition of actin monomers to actin filament barbed ends, inhibit both the morphological alterations and actin assembly (3, 8). Recent investigations have established that although about half of the actin in resting platelets is unpolymerized, stored as 1:1 complexes with β4-thymosin (37, 38) or profilin (28, 29), the remainder of the actin in resting platelets is polymeric, consisting of filaments of ~1 μm in length. These filaments are crosslinked at high angles by

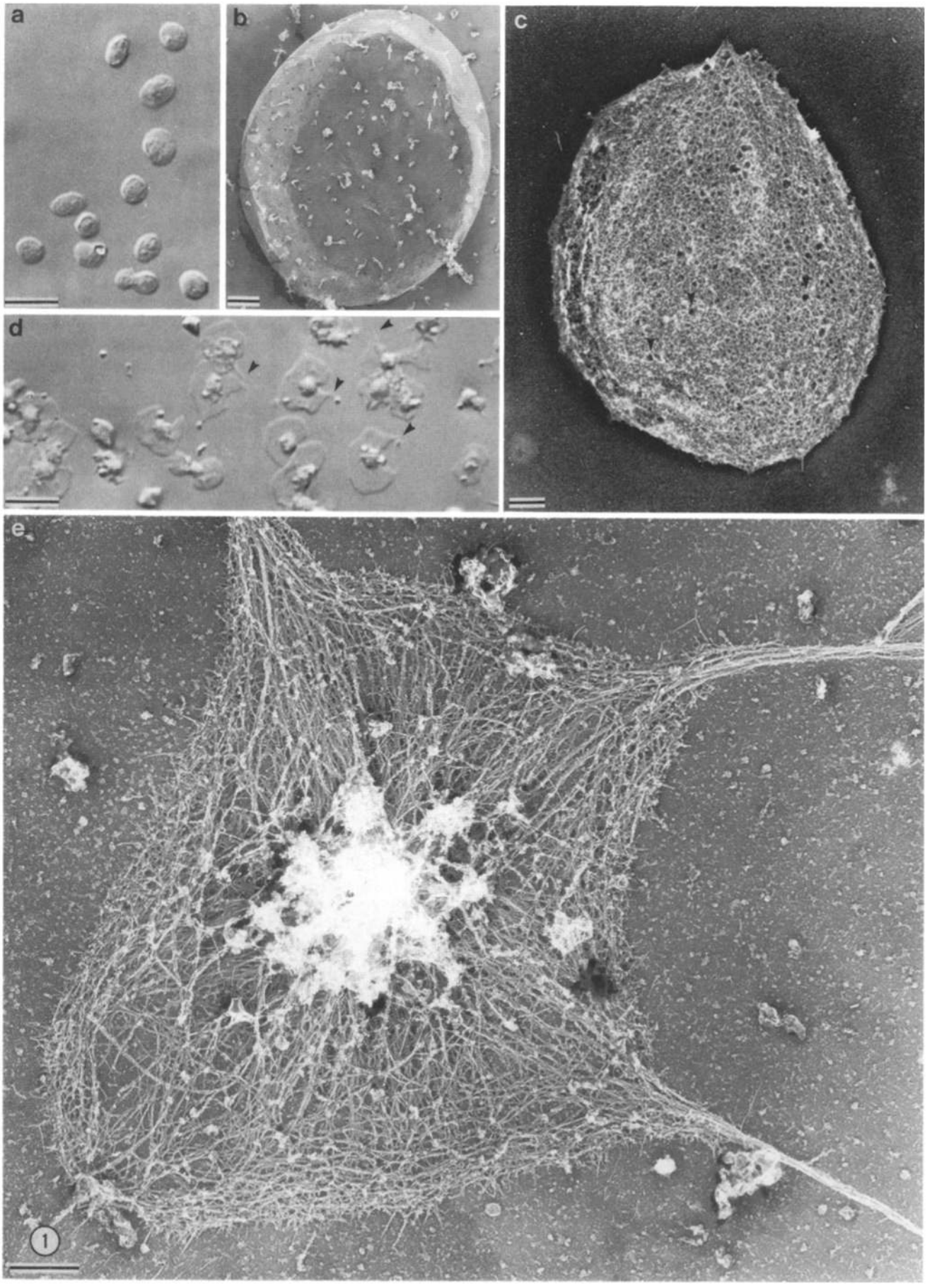
a
b
c
d
e
1

actin-binding protein (ABP)[1] within the platelet substance and bind to a dense spectrin-rich shell that laminates the plasma membrane (4, 10–12). This article provides new details about the architecture of actin in the activated platelet and addresses the mechanism of how remodeling of the resting structure leads to the configuration characteristic of the activated cell. It describes experiments that also examine the particular role of the actin filament severing and barbed-end blocking protein, gelsolin, in this remodeling.

Materials and Methods

Preparation of Resting Platelets

Human blood from healthy volunteers, drawn into 0.1 vol of Aster-Jandl anticoagulant, was centrifuged at 110 *g* for 10 min. The platelet-rich plasma was gel-filtered through a Sepharose 2B column equilibrated and eluted with a solution containing 145 mM NaCl, 10 mM Hepes, 10 mM glucose, 0.5 mM Na_2HPO_4, 5 mM KCl, 2 mM $MgCl_2$, and 0.3% BSA, pH 7.4 (platelet buffer). 2 U/ml apyrase was added to the platelet suspension and the cells were left standing for 60 min at 37°C as previously reported (12, 15). To maintain cytosolic calcium at or below its resting level during cell activation, cells were loaded with 30 μM Quin-2AM during minutes 30–60 of the rest period. The effect of Quin-2 was reversed by the addition of 1 mM $CaCl_2$ to the bathing media before centrifugation of the Quin-2-loaded cells onto the coverslips or after the cells had been attached and formed filopodia on the coverslip. Glass-adherent, Quin-2-loaded cells were also treated with 1 mM $CaCl_2$ and 20 nM of the ionophore A23187 for 15 s and then detergent permeabilized. In some cases, platelets were used directly from platelet-rich plasma by diluting it 1:20 with platelet buffer containing, in addition, 0.1 mM EGTA and 2 U/ml apyrase. The diluted cells were incubated for 30 min at 37°C to insure a resting state.

Activation of Platelets

Platelet suspensions were activated by the addition of 1 U/ml of thrombin (hereafter called thrombin-activated) for 15–30 s in studies of nucleation activity. Activation was terminated by permeabilizing the cells as detailed below. Glass activation was used for the morphological studies. Cells were glass-activated by centrifugation onto polylysine-coated glass coverslips at 250 *g* for 5 min. Coverslips were placed in the bottom of multiwell plates (24 or 96 wells), covered with 0.25 ml of platelet suspension, and centrifuged at 37°C in a Sorvall HB-6000 centrifuge using multiwell carriers.

Fluorescence Measurement of Actin Assembly in Lysates from Resting and Activated Cells

The effect of cell lysates on the rate and extent of pyrene-labeled rabbit skeletal muscle actin was determined as described previously (13). Suspensions of resting or thrombin-activated cells at concentrations of 1.4×10^8/ml were permeabilized by the addition of 0.1 vol of 60 mM Pipes, 25 mM Hepes, 10 mM EGTA, 2 mM $MgCl_2$, 0.75% Triton, and 42 nM leupeptin, 10 mM benzamidine, and 0.123 mM aprotinin to inhibit proteases (40). 100 μl of detergent lysate was added to 190 μl of 100 mM KCl, 2 mM $MgCl_2$, 0.5 mM ATP, 0.1 mM EGTA, 0.5 mM dithiothreitol, and 10 mM Tris, pH 7.0, and the polymerization rate assay was started by the addition of monomeric pyrene-labeled rabbit skeletal muscle actin to a final concentration of 2 μM. The relative contribution of nuclei with barbed or pointed ends in the cell lysates was determined by adding 2 μM cytochalasin B to the pyrene nucleation assay system. Pyrene actin assembly onto actin filament nuclei has been shown to be completely inhibited at the barbed end by 2 μM cytochalasin B. Cytochalasin B inhibitable activity in the nucleation assay is, therefore, defined as "barbed" end assembly. Activity not inhibited by cytochalasin B is considered pointed end assembly. The stability of nucleation activity in cell lysates was tested by comparing the stimulatory effect of fresh lysate on actin assembly with lysates allowed to stand for 30 s to 30 min at 37°C before addition to the assembly assay. To determine if the measured stimulation of actin assembly and its decay with time was due to the growth of pyrene-actin addition onto cellular filaments subject to depolymerization in the diluted lysate, 0.1 μM phalloidin or phallacidin was added to the cell lysates during their preparation to stabilize the filaments. As shown in Results, all nucleation activity present in resting and activated cells was associated with the detergent-insoluble cytoskeleton. However, we also determined that the soluble phase from cells permeabilized with detergent in the presence of EGTA contained calcium-dependent nucleation activity. Detergent lysates from resting and thrombin-activated cells (30 s, 1 U/ml) were centrifuged at 10,000 *g* for 2 min at room temperature in a microcentrifuge. The supernatant was removed and added to the pyrene-based nucleation assay in the presence of 1 mM EGTA or $CaCl_2$. The amount of pointed end activity in these soluble extracts was determined by adding a final concentration of 2 μM cytochalasin B to the pyrene-actin assembly assay.

The effect of inhibiting barbed end actin assembly in thrombin-activated cells before detergent lysis on the amount of nucleation activity was determined by preincubating resting platelet suspensions with 2 μM cytochalasin B for 5 min. Because it was necessary to wash out the cytochalasin B from some of the cytoskeletons before addition of the cell lysates to the pyrene assembly assay, the cells were first attached to glass coverslips while still in the presence of cytochalasin B. This was accomplished by sedimenting 0.3 ml of cell suspension onto a 12-mm round glass coverslip for 5 min at 250 *g*. Individual coverslips were removed, treated with thrombin for 15 s in the presence of cytochalasin B, permeabilized with 1× PHEM-Triton buffer containing 2 μM cytochalasin B for 15 s, and then washed in PHEM buffer in the presence or absence of cytochalasin B. Coverslips were then immediately assayed for their ability to promote actin filament assembly as previously described by us using glass adherent macrophage cytoskeletons (13).

Morphological Studies

LIGHT MICROSCOPY

Resting platelets were fixed for 10 min in suspension by the addition of 1 vol of 2% glutaraldehyde. They were attached to polylysine-coated coverslips by centrifugation at 250 *g* for 5 min. Glass-activated platelets were sedimented onto the coverslips in an identical fashion but without fixative.

1. *Abbreviations in this paper*: ABP, actin-binding protein; OCS, open canalicular system.

Figure 1. Comparison of the structure of resting and activated platelets and their cytoskeletons. (*a–c*) Structure of the resting platelet and its cytoskeleton. (*a*) Morphology of resting cells in the light microscope. Cells were fixed in suspension, attached to glass coverslips by centrifugation, and photographed using DIC optics. The bar is 5 μm. (*b*) Surface topology of a resting platelet. The surface of the cell is smooth except for pits that are the external openings of the OCS of the resting cell. A few pits are labeled with white arrows. The bar is 0.5 μm. (*c*) Representative cytoskeleton from a resting cell. As reported in reference 12, the resting platelet cytoskeleton has a dense membrane skeletal coat that covers and obscures the underlying three-dimensional actin cytoskeleton. This membrane skeleton coat retains residual OCS openings (*black arrowheads*). The bar is 0.5 μm. (*d–e*) Structure of glass-activated platelets. Cells were glass-activated by sedimenting them onto polylysine-coated coverslips in a centrifuge at 250 *g* for 5 min. (*d*) Glass-activated cells (5 min) flatten and spread using both lamellipodia and filopodia. Many lamellae also contain filopods (*arrowheads*). This DIC photograph is the same magnification as in *a*. The bar is 5 μm. (*e*) Representative cytoskeleton from a glass-activated cell (2 min). Two zones of actin filament assembly are apparent. One zone is composed of long filaments that run outward from the cytoskeletal center into the filopods. This zone is hereafter called filopodial bundles. Microtubules may also enter some of the filopods. The second zone is an orthogonal network of short actin filaments that fills lamellipods. This is termed the "lamellipodial network." The middle of the cytoskeleton can be seen to be filled with electron-dense material after activation. The bar is 0.5 μm.

Coverslips were maintained at 37°C for 2 min after centrifugation and then fixed by removing the solution bathing the coverslip and replacing it with platelet buffer containing 4% glutaraldehyde for 10 min. Coverslips were washed with water, dried, mounted on microscope slides using poly-mount (Polysciences, Inc., Warrington, PA) and photographed using DIC optics in an IM-35 inverted microscope (Carl Zeiss, Inc., Thornwood, NY).

ELECTRON MICROSCOPY

Rapid Freezing and Freeze-drying. Platelets were glass-activated by surface contact. Solutions of 250 μl of platelets in suspension were placed in wells of a 96-well microtiter plate, each containing a polylysine-coated coverslip, and the plate was centrifuged at 1,450 *g* for 5 min at 37°C. Some cells were fixed with 1% glutaraldehyde to study their surface topology. Cells fixed in a resting state were also applied to coverslips for comparison to the activated cells. Replicas of intact resting and activated cytoskeletons were prepared by permeabilizing resting cells in suspension or glass-activated cells with PHEM-0.75% Triton X-100 buffer (40) containing 5 μM phallacidin, protease inhibitors, and 0.1% glutaraldehyde for 2 min (12). The cytoskeletons were washed in PHEM buffer containing 0.1 μM phalloidin and fixed in PHEM containing 1% glutaraldehyde for 10 min. Coverslips of fixed cells and cytoskeletons were extensively washed with distilled water, rapidly frozen, freeze-dried, and rotary coated with metal and carbon in a Cressington CFE-50 freeze-fracture apparatus (Cressington Scientific Instruments, Ltd., Watford, England).

Labeling of Cytoskeletons with Myosin S1 and Exogenous Actin. Coverslip-adherent cytoskeletons prepared as described above in the presence of phallacidin but not fixative were incubated with 5 μM skeletal muscle myosin S1 in PHEM for 10 min at room temperature, washed twice with PHEM buffer, and then fixed with a solution of 0.2% tannic acid, 1% glutaraldehyde, and 10 mM sodium phosphate buffer, pH 7.5. They were rapidly frozen, freeze-dried, and metal coated as described above. The locations of nucleation sites in activated platelet cytoskeletons from glass-activated cells were determined by assembling skeletal muscle actin at concentrations of 8 and 10 μM onto the ends of S1-decorated platelet actin filaments. S1 was adhered to platelet actin filaments by treating S1-labeled cytoskeletons with 1 mM *N*-ethylmaleimide in PHEM buffer for 5 min. The assembled filaments were stabilized by the addition of equilimolar phallacidin, washed twice with PHEM buffer, and fixed with 0.2% tannic acid, 1% glutaraldehyde, and 10 mM sodium phosphate buffer, pH 7.5.

Gold Labeling of Cytoskeletons from Resting and Activated Cells with Antibodies to Gelsolin. Colloidal gold particles, 5 and 8 nm in diameter, were prepared with tannic acid (44) and coated with affinity-purified rabbit anti-goat IgG that had been absorbed with human IgG. The affinity-purified goat anti-rabbit macrophage gelsolin IgG has been characterized in previous studies (12, 14). To label glass-adherent cytoskeletons, residual fixative was blocked with 0.1% sodium borohydride in PHEM buffer, and the coverslips containing cytoskeletons were washed twice in PBS and twice in PBS containing 1% BSA, pH 8.2. Coverslips were covered with 25 μl of primary antibodies at a concentration of 10 μg/ml, incubated for 1 h at 25°C, and washed three times with PBS/BSA. Coverslips were then incubated for 1.5 h with a 1:20 dilution of rabbit anti-goat IgG–colloidal gold particles, washed three times in PBS/BSA and three times in PBS, and fixed with 1% glutaraldehyde in 10 mM sodium phosphate buffer for 10 min. Fixed specimens were washed extensively with distilled water, rapidly frozen, freeze-dried, and rotary coated with 1.2 nm of tantalum-tungsten at 45° and 3.0 nm of carbon at 90° without rotation as previously described (12). Thin sections of Lowicryl-K4M-embedded resting cytoskeletons were labeled with antigelsolin IgG and 5 nM colloidal gold as previously described (16). No gold labeling was found when primary IgG was omitted, when preimmune IgG was used instead of antigelsolin IgG, or when gelsolin-absorbed primary antibody was used (16).

Results

Structure of the Resting and Activated Platelet Cytoskeleton

Fig. 1 shows aspects of the structure of resting platelets and a representative cytoskeleton and compares them with changes occurring in cells and a cytoskeleton from a glass-activated platelet. Fig. 1, *a–c* reveals some new features of the structure of the resting cell. The structure of the cytoskeleton of the resting platelet has been previously described (2, 12), but some important features are shown here for comparison with glass-activated cells and their underlying cytoskeletons. Resting platelets are disks that, when centrifuged onto glass coverslips, attach along their flat axis (Fig. 1 *a*). The surface of a resting cell is shown in Fig. 1 *b*. It is relatively flat and featureless except for numerous pits that open to the canalicular system (OCS) of these cells (50, 52). These openings are also preserved in the membrane skeleton of resting cells permeabilized with detergent (Fig. 1 *c*). As reported previously, the membrane skeleton of the resting platelet includes a dense spectrin-rich shell that covers an underlying three-dimensional actin filament core (see below, Fig. 12). Long actin filaments radiate outward from the cell center and interconnect with the membrane skeleton on their ends and sides through spectrin tetramers and ABP/GPIb$_{\alpha\beta}$/IX complexes (2, 9, 12, 36).

Figs. 1, *d* and *e* and 2 show the surface of representative platelets spread on the surface of a glass coverslip and cytoskeletal preparations from these cells. Platelets spread circumferentially by extension of 1–5-μm-long filopods and broad sheets of thin lamellae (1). Inspection of the surface of spread cells reveals that they no longer have surface pits (Fig. 2 *b*). In accordance with the work of many laboratories (22, 30, 32, 49), a dramatic remodeling of the cytoskeleton accompanies the extension of cellular processes. In rapidly frozen and freeze-dried specimens, a reproducible reordering of cytoskeletal actin occurs as they spread on the glass surface and two distinct zones of new actin filament assembly are found. Labeling of cytoskeletons from activated cells with skeletal myosin S1 demonstrates that almost every 10-nm-diameter filament in the cytoskeleton of an activated platelet is actin (Fig. 3). Filopods contain bundles of long fibers (Fig. 1 *e*, 2 *c*, and 3) that radiate in parallel out from the center of the cytoskeleton. The bundle fibers originate from diverse points within the internal actin filament core and converge at the base of the filopodia (Figs. 1 *d* and 2). These are hereafter referred to as filopodial bundles. A second type of filament organization is within the lamellae. Filaments within lamellae are short and ordered into space-filling orthogonal networks (Fig. 1 *e* and stereo micrographs in Fig. 2). These are referred to as lamellipodial networks.

Actin Nucleation Activity in Resting and Activated Cells

To understand how new filament assembly is initiated during cell activation, the nature and amount of nucleation activity in detergent lysates from resting and thrombin-activated cells was characterized using a pyrene-actin assembly system in vitro. As shown in Table I, lysates of resting cells permeabilized with Triton X-100 had only a small stimulatory effect on the rate at which pyrene-actin assembled in solutions containing 0.1 M KCl and 2 mM $MgCl_2$. This small increase in the rate of actin assembly by resting lysates was probably due primarily to the addition of pyrene monomers onto the slow-exchanging filament ends (pointed end of S1-labeled fibers), because addition of 2 μM cytochalasin B to lysates from resting cells, which blocks exchange at the high affinity ends, had only a small effect on the amount of nucleation activity measured in the pyrene assay. From the kinetics and extent of pyrene assembly and rates of addition of monomers to the filament ends, 2,000 pointed filament ends are present in a

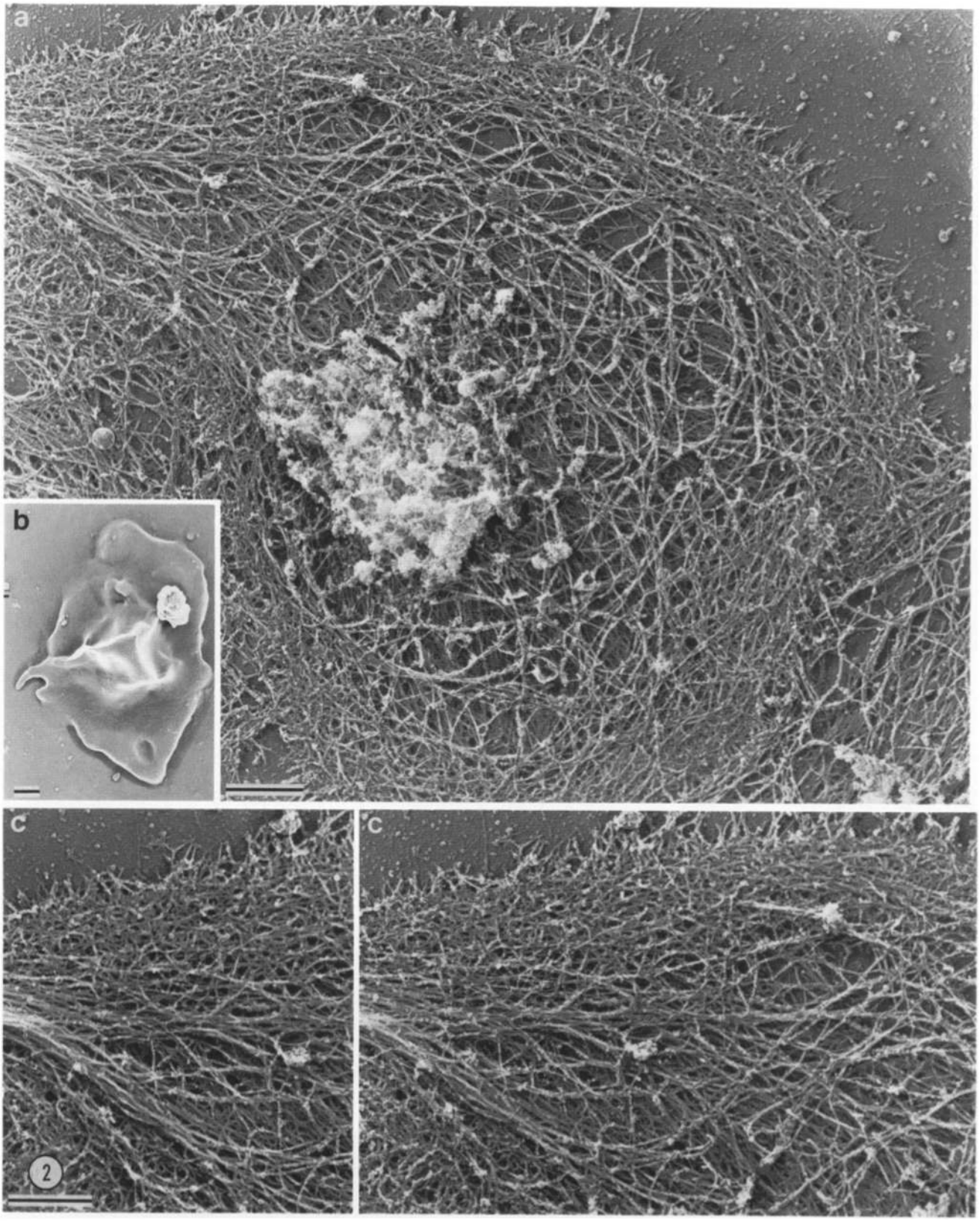

Figure 2. Structure of a cytoskeleton from a glass-activated cell. (*a*) Representative cytoskeleton from a cell incubated on glass for 5 min. Filaments comprising the lamellipodial network are longer than those in Fig. 1 *e*. Both filopodial bundles and lamellipodial networks are apparent. (*b*) Surface structure of a glass-activated cell. Spreading is accompanied by the loss of OCS pits from the cell surface. (*c*) Paired electron micrographs (±10° of tilt) showing a filopodia to be cored by filaments that originate in the cytoskeletal center and lamellipodia networks to be composed of short (≤0.5 μm) filaments. The bars are 0.5 μm.

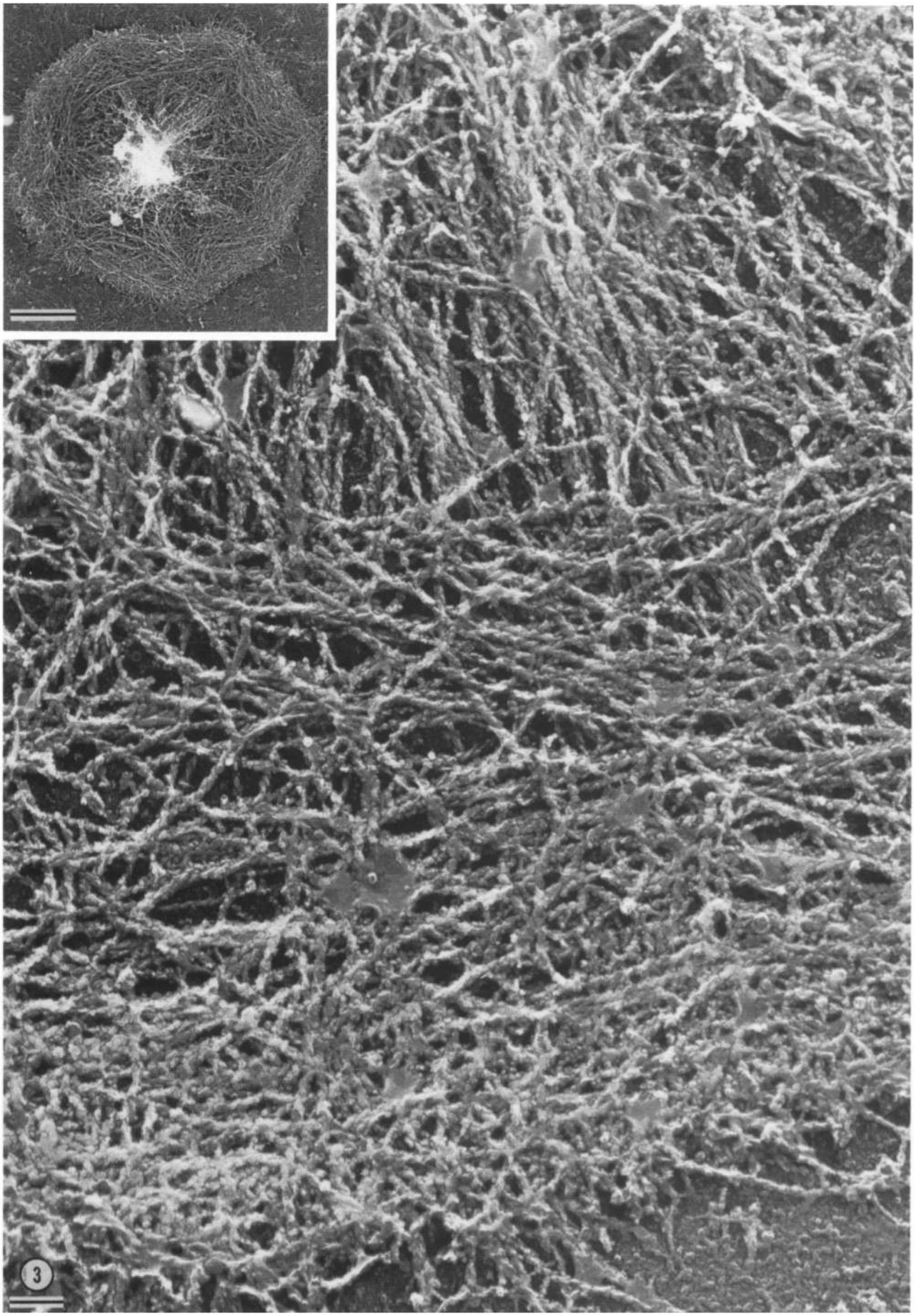
3

Table I. Calcium-insensitive Cytoskeletal Nucleation Activity

Treatment	Assembly rate (pointed end)	Assembly rate (barbed end*)	Subunits added to pointed ends‡	Subunits added to barbed ends§	Pointed nuclei/platelet	Pointed nuclei/platelet
	$nM\ s^{-1}$	$nM\ s^{-1}$	$\times 10^{10}\ s^{-1}$	$\times 10^{10}\ s^{-1}$		
Resting	0.21 ± 0.04	0.04 ± 0.02	3.7 ± 0.70	0.7	2,000 ± 380	50 ± 25
Activated	0.24 ± 0.02	0.58 ± 0.03	4.3 ± 0.35	10.4	2,500 ± 200	410 ± 15

Comparison of the actin nucleation capacities of detergent lysates from resting and thrombin-activated platelets. Gel-filtered platelets were suspended to a concentration of 1.4×10^8/ml in platelet buffer, rested for 30 min at 37°C, and then treated with or without 1 U/ml of thrombin for 15 s. The cells were permeabilized by the addition of 0.1 vol of 10× PHEM buffer (40) containing 0.75% Triton X-100 and protease inhibitors. 110 μl of platelet lysate was added to 180 μl of 0.1 M KCl, 0.5 mM ATP, 2 mM $MgCl_2$, 0.5 mM β-mercaptoethanol, and 2 mM Tris, pH 7.0. The rate assay was started by the addition of pyrene-labeled actin monomers to a final concentration of 2 μM. The final volume was 0.3 ml. 2 μM cytochalasin B was added to determine the amount of total activity related to the barbed filament end. There were 1.4×10^7 platelets per assay. Data are expressed as mean ± SD, $n = 4$.

* The barbed end assembly rate is calculated by subtracting the assembly rate in the presence of 2 μM cytochalasin B from the assembly rate in the absence of cytochalasin B.

‡ Initial pointed end addition rate in 2 μM actin solution was 1.2 subunits s^{-1}.

§ Initial barbed end addition rate in 2 μM actin solution was 18 subunits s^{-1}.

resting cell. Lysates from cells activated with 1 U/ml of thrombin for 15–30 s before permeabilization, however, increased the pyrene-actin assembly rate three- to four-fold relative to resting lysates (Table I and Fig. 4). In contrast to the resting lysates, the stimulatory effect in these lysates was abolished by the addition of 2 μM cytochalasin B to the actin assembly assay (Table I). Since cytochalasin B blocks new actin assembly in both intact, thrombin-activated platelets (3, 8) and in lysates from thrombin-activated cells, filament assembly in platelets must occur predominantly on the fast growing end of filaments. Depending on the experiment, 410–570 barbed ends would have been required on average in each platelet to increase the rate of actin assembly by the determined extents (Table I and Fig. 4).

Before centrifugation, lysates increased the actin assembly rate by 1.528 ± 0.11 nM s^{-1} (mean ± SD) relative to actin alone. Centrifugation of lysates at 10,000 *g* for 2 min, which sediments aggregates of cellular actin fibers but not individual actin filaments, removed 99% of the nucleation activity induced by thrombin. This result indicates that all barbed end nucleation activity measured in EGTA-containing buffer was associated with the low-speed sedimentable platelet cytoskeleton.

In all of the nucleation experiments described above, the calcium ion concentration was low because all solutions contained EGTA to chelate calcium. Although raising the calcium concentration of assay solutions into the micromolar range by addition of sufficient $CaCl_2$ had no effect on the barbed end nucleation activity that was sedimentable in lysates of thrombin-activated platelets (data not shown), the soluble fraction remaining after removal of cytoskeletons also contained a large amount of calcium-dependent actin nucleation activity (Table II). This activity was, however, in contrast to the calcium-insensitive sedimentable activity, completely unaffected by 2 μM cytochalasin B, demonstrating that it promotes actin assembly only in the pointed direction. No calcium-activated soluble nucleation activity was detectable in lysates from resting cells.

Evidence That Most of the Nuclei in Detergent Lysates from Activated Cells Are Short Actin Filaments

Fig. 4 *a* demonstrates that the amount of nucleation activity in lysates of thrombin-activated cells decayed rapidly. When lysates of thrombin-activated cells were assayed immediately after addition of detergent, ~570 barbed ends were available per platelet cytoskeleton to stimulate filament assembly. If lysates were maintained at 37°C for 2 min before their addition to the pyrene-actin assembly assay, ~40% of the original nucleation activity was lost. Nucleation activity contained in lysates was exhausted in ~10–20 min. This result suggested that most of the nucleation activity in lysates from activated cells resulted from addition of pyrene subunits onto short actin filaments. In the diluted lysates these filaments depolymerized, causing nucleation activity to decay with time. It can be estimated from published actin filament end disassembly rates (17) that the main source of actin nucleation activity in these lysates is filaments ≤0.3 μm in length (also see below). Fig. 4 *b* shows that the addition of 0.1 μM phalloidin to detergent lysates stabilized the nucleation activity. This result demonstrates that short actin filaments are the source of most of the nucleation activity in activated cell lysates.

Location of Cytoskeletal Actin Nucleation Activity

Sites available for filament assembly were localized in glass-activated platelets. The actin filaments in cytoskeletons from activated cells were coated with myosin S1 fragments, allowing identification where new actin filaments assembled after addition of monomeric actin to the decorated cytoskeletons. As shown in Fig. 5, such new filaments, detectable by their lack of an S1 coating, grew at the cytoskeletal margin off the

Figure 3. Demonstration by myosin S1 labeling that cortical 10-nm filaments are actin. Glass-activated cells were permeabilized as detailed above and incubated with 5 μM rabbit skeletal muscle S1 in PHEM buffer for 5 min, washed twice in PHEM buffer, fixed with 0.2% tannic acid and 1% glutaraldehyde in 10 mM sodium phosphate buffer, pH 7.0, rapidly frozen, freeze-dried, and metal-coated with 1.2 nm of tantalum-tungsten and 2.5 nm of carbon. The bar is 0.1 μm. (*Inset*) Low magnification of S1-labeled platelet demonstrating that the cytoskeleton remains intact. The bar is 1 μm.

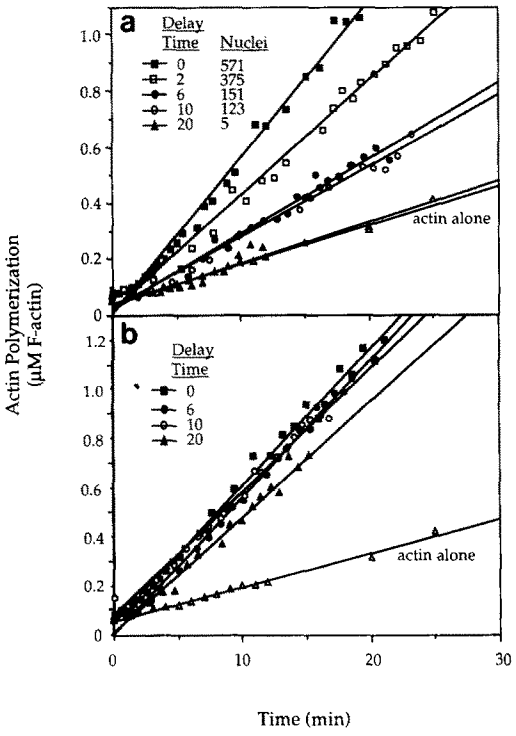

Figure 4. Thrombin-stimulated nucleation activity decays unless actin in the lysates is stabilized using phalloidin. Resting platelets in suspension (140,000/μl) were activated by the addition of 1 U/ml of thrombin for 15 s and then permeabilized with 0.1 vol of 10× PHEM buffer containing 0.75% Triton X-100 and protease inhibitors. (*a*) Lysates were prepared by detergent treatment and then incubated at 37°C for the indicated times before being assayed for nucleation activity (*closed squares*, 0; *open squares*, 2 min; *closed circles*, 6 min; *open circles*, 10 min; *closed triangles*, 20 min). The rate at which 2 μM pyrene-actin assembled in the presence or absence of lysates is shown. The number of free barbed ends per platelet necessary to accelerate the rate by the determined amount are indicated. (*b*) Effect of phalloidin treatment on the stability of nucleation sites in thrombin-activated lysates. Platelets were activated with thrombin and lysed with detergent as in *a* except that 0.1 μM phalloidin was included in the PHEM-Triton lysis buffer. The symbols are the same as in *a*.

ends of the short filaments. The interior of the cytoskeleton did not support filament growth.

Evidence for the Role of Calcium in Cytoskeletal Rearrangements Occurring with Platelet Activation

Quin-2-loaded Platelets Attach to Glass, Extend Filopodia, but Do Not Spread. Loading platelets with 30 μM Quin-2AM had no effect on the structure of the resting cells

Table II. Calcium-sensitive Soluble Nucleation Activity

Treatment	2 μM CB	Assembly rate*	Subunits added to pointed ends‡	Pointed nuclei/platelet
		nM s⁻¹	*×10¹¹ s⁻¹*	
Resting	+	ND	-	-
Resting		ND	-	-
Activated	+	0.55 ± 0.02	1.0 ± 0.05	5,000 ± 250
Activated		0.54 ± 0.03	0.97 ± 0.05	4,850 ± 243

Calcium-dependent soluble nucleation activity in activated platelet lysates. Lysates were prepared from resting thrombin-treated cells with detergent and centrifuged in a Sorvall Microspin 12S at 13,000 rpm for 1 min. Nucleation activity remaining in the supernatant after removal of the cytoskeletal fraction was determined. Centrifugation of lysates removed all cytoskeletal-associated nucleation activity from the resultant supernatants. There were 2.0×10^7 platelets per assay. The data are expressed as mean ± SD, $n = 4$. ND, not detectable.

* The barbed end assembly rate is calculated by substracting the assembly rate in the presence of 2 μM cytochalasin B from the assembly rate in the absence of cytochalasin B.

‡ Initial pointed end addition rate in 2 μM actin solution was 1.2 subunits s^{-1}.

observed in the light microscope or cytoskeletons prepared from these resting cells (data not shown). However, the morphologies of glass-activated cells differed from untreated cells spreading on coverslips. As shown in Fig. 6 *a*, platelets loaded with Quin-2 and then glass activated extend filopodia but not lamellipodia. Filopodia were 2–5 μm in length, thicker in diameter relative to those from control cells, and had bulbous endings (Fig. 7). Although filopodia extended from these cells, the cell shape remained discoid with dimensions near those of the resting cell (Fig. 6, *a–c*). In the electron microscope, the surface of intact cells retained the pits of the OCS (Fig. 6, *b*, *arrows*). While most of the cells had filopodia, some other morphologies were also apparent (Fig. 6 *a*). Most glass-activated Quin-2-loaded platelets extended one prominent filopod, but a few simply elongated or made small spherical protrusions at their margins. As detailed below, these different morphologies resulted from related cytoskeletal actin rearrangements. If Quin-2-loaded cells were bathed in medium containing millimolar calcium, normal spreading of cells resulted on the glass surfaces (i.e., cells spread both lamellipodia and filopodia [see Fig. 9]).

When observed in the electron microscope, cytoskeletons prepared from Quin-2-loaded and glass-activated cells lack lamellipodial networks at their margins. Instead, these cytoskeletons are composed exclusively of long filaments running parallel to the cell margin. These filaments appear to derive from filaments originating in the cell center which turn and run along the cytoskeletal edges (Fig. 6, *c–e*). Filopodia in cytoskeletons from Quin-2-loaded cells are filled with actin filaments originating near the middle of the cytoskeleton (Fig. 6 *d*), but these filaments do not end near the tips of the filopodia as in control cells. Instead, these fila-

Figure 5. Localization of nucleation sites in cytoskeletons from platelets spread on glass coverslips. Platelet cytoskeletons coated with myosin S1 which was stabilized with 1 mM *N*-ethylmaleimide were incubated for 1 min with 10 μM rabbit skeletal muscle actin, washed with PHEM buffer containing 5 μM phallacidin, fixed, rapidly frozen, freeze-dried, and coated with 1.2 nm of tantalum-tungsten and 2.5 of carbon. (*a*, *b*) Low magnification micrographs of representative cytoskeletons showing growth of actin filaments from the cytoskeletal margins. The lines demarcate the margins of the S1-labeled cytoskeleton. New filament growth extends outward from these S1-labeled margins. The bar is 0.5 μm. (*c*) Paired micrographs of cytoskeletons treated as described above. Unlabeled actin filaments extend from the margins of the S1-labeled cytoskeleton. Some filaments grow upward from the lamellipodial network. Unlabeled filaments are not found in the cytoskeletal interior. The bar is 0.2 μm.

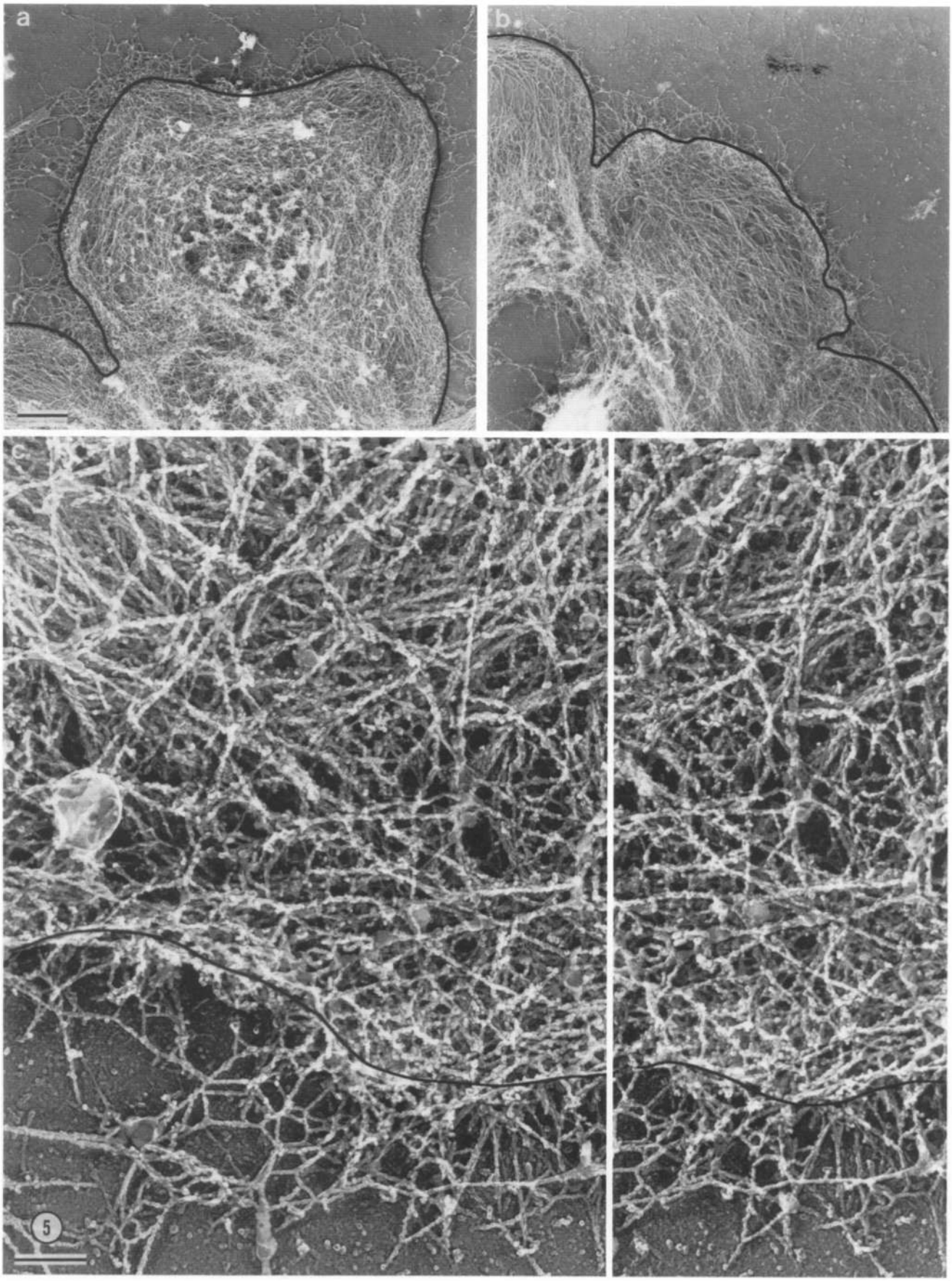
a
b
c
5

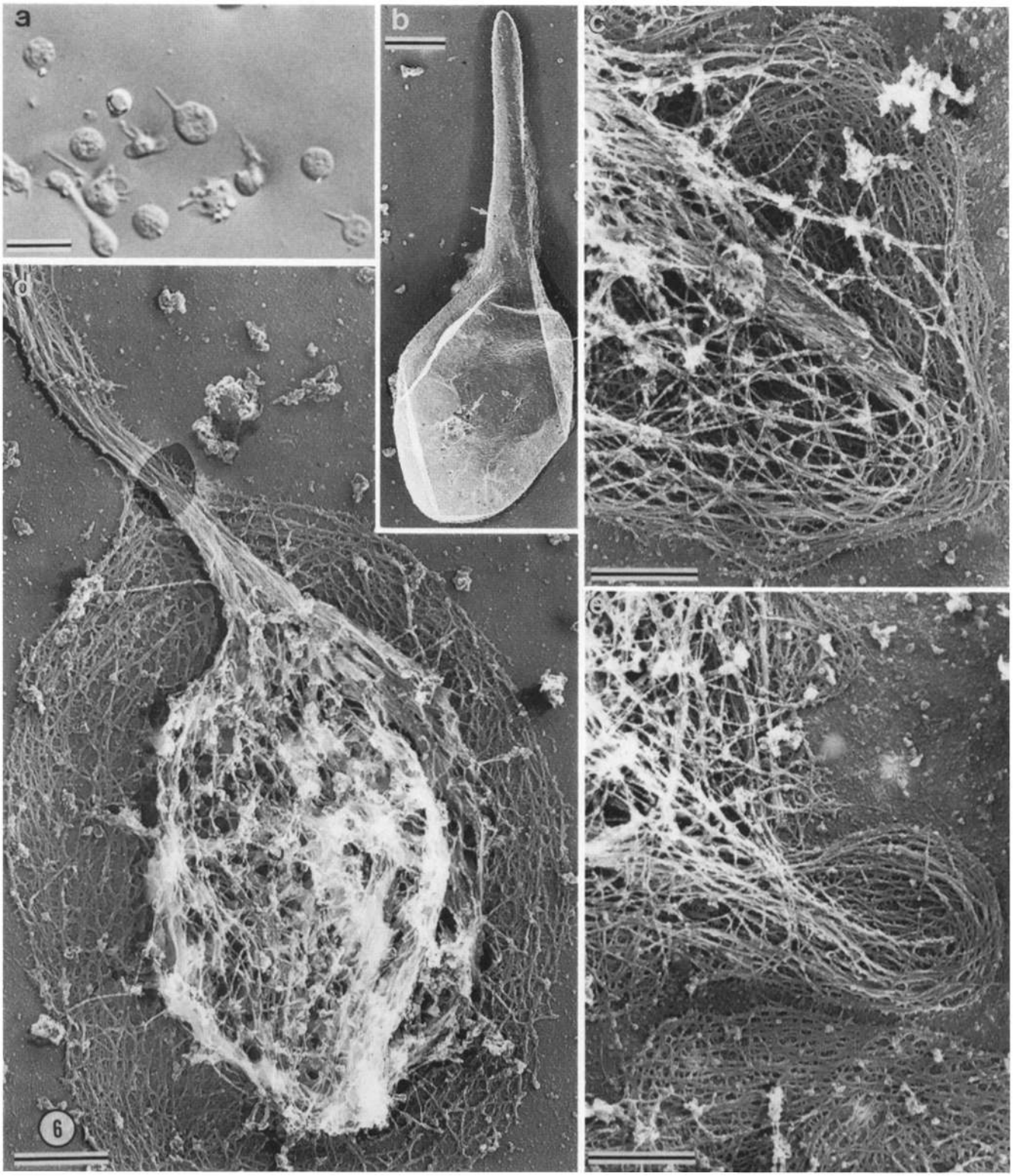

Figure 6. Structure of platelets and their underlying cytoskeletons preloaded with 30 μM Quin-2 for 30 min at 37°C (7) before glass activation. (*a*) DIC light micrograph of Quin-2-preloaded, glass-activated cells. These cells spread abnormally, extending filopodia having bulbous endings (compare with Fig. 1 *d*; the magnification is the same). Some cells elongate slightly while others have small blebs on their surface. The bar is 5 μm. (*b*) Structure of the surface of an intact Quin-2-loaded and glass-activated cell. The cell surface retains the pits that are the external openings of the OCS (*white arrow*). The bar is 0.5 μm. (*c–e*) Representative cytoskeletons prepared from Quin-2-loaded and glass-activated cells. Cells were permeabilized with PHEM-Triton buffer containing protease inhibitors and 5 μM phalloidin. These micrographs demonstrate that the radial filaments in these cells remain long and unfragmented. These filaments radiate outward from the center of the cell. When they approach the cell edge they turn and run parallel to it. (*c*) Cytoskeleton having a single filopod. (*d*) Cytoskeleton from an elongated cell that lacks filopodial extensions. Note that the actin filaments have formed a loose bundle inside the cytoskeleton. This bundle runs to the cytoskeletal margin where filaments forming it branch off and run along the cell edge or reenter the cytoskeletal interior. (*e*) Structure of actin filaments in a small bleblike protrusion on the edge of a cytoskeleton. The bars in *c–e* are 0.5 μm.

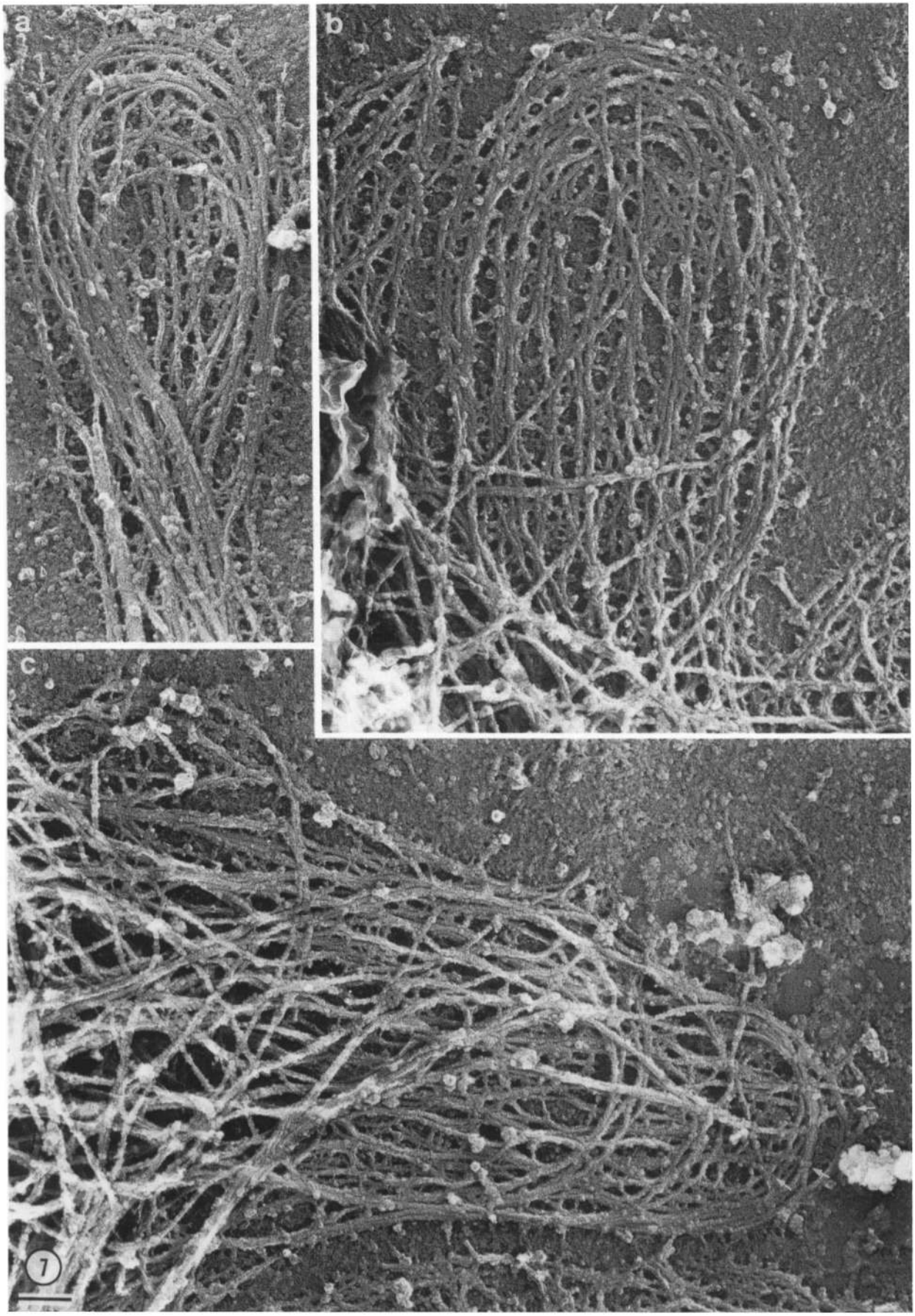

Figure 7. Electron micrographs showing the organization of actin filaments in the tips of the cytoskeletal protrusions formed after Quin-2-loaded cells are glass-activated. The most prominent feature of each micrograph is that cortical filaments are continuous in the blebs and make loops inside them. In each micrograph a small number of long, straight filaments are also present that run outward from the cytoskeleton into the protrusion and end (*white arrows*). The bar is 0.1 μm.

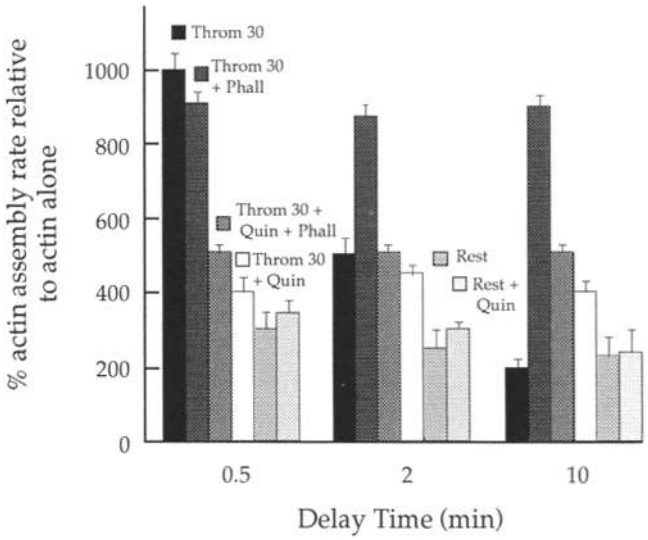

Figure 8. Effect of Quin-2 preloading on the amount of nucleation activity in lysates from resting and thrombin-activated platelets. Gel-filtered platelets were divided. One group of cells was loaded with 30 μM Quin-2 AM for 30 min at 37°C (7). Nucleation activity in lysates from unstimulated cells (resting + Quin-2) and in lysates from cells exposed to 1 U/ml of thrombin for 15 and 30 s were determined immediately and at 2- and 10-min lag times after detergent permeabilization. Nucleation activities were also determined in lysates prepared from cells permeabilized with PHEM-Triton containing 0.1 μM phalloidin. The actin polymerization rate is expressed as a percentage of that relative to pyrene-actin assembly alone. These data are expressed as the mean of four individual experiments ± SD.

ments make U-turns and run back into the body of the cytoskeleton (Fig. 7). These filament loops, therefore, appear to produce the bulbous enlargements at the ends of filopodia in these cells. Not all actin fibers entering filopods make U-turns. A few of the filaments within filopodia end near their tips (arrows in Fig. 7). Examination of cytoskeletons from cells displaying simply an elongated shape without a filopod reveals them to have internal bundles of filaments (Fig. 6 *c* and 7). Fibers coming off the ends of these bundles turn and run in parallel with filaments in the cytoskeletal margins or turn and run back toward the middle of the cytoskeletons instead of exiting to form filopodia. Cytoskeletons of bleb forms also share these features (Figs. 6 *e* and 7 *b*). Blebs at the cytoskeletal edges are composed of loops of actin filaments with some underlying straight filaments.

Quin-2 Loading Diminishes Thrombin-stimulated Nucleation Activity. Nucleation activity in lysates from Quin-2-loaded and control cells was compared after thrombin activation (Fig. 8). Lysates from activated cells loaded with Quin-2 had only 28% of the nucleation activity of lysates from untreated and activated cells when assayed immediately. When directly compared, the total number of nuclei was equivalent to that remaining in control lysates incubated for 2 min before addition to the assembly assay. Although the total nucleation activity was reduced, its stability was increased in lysates of Quin-2-chelated, thrombin-activated cells. Nucleation activity in the detergent lysates from Quin-2-loaded cells was more stable, and no loss in its activity occurred in lysates incubated for as long as 10 min before addition to the assembly assay. In contrast to lysates from unchelated cells, phalloidin had no effect on the nucleation activity in lysates from Quin-2-loaded cells. The stability of actin filament nuclei in the Quin-2-loaded cells could result either from their being considerably longer in length compared with control cells or from their being coated with proteins that retard depolymerization. The former alternative finds support in the electron microscope where the periphery of Quin-2-loaded and activated cells are replete with long fibers (Figs. 6 and 7). Filaments of lengths $\geq$1.5 μm would have survived to nucleate in the assay.

The above experiments have shown that long actin filaments preexisting in resting platelets shorten in a calcium-dependent fashion during cell activation with thrombin or glass stimuli and that these short filaments then become templates for the assembly of lamellipodial networks. Two possibilities exist for the formation of this short filament population during cell activation. Filaments forming the resting cytoskeleton could be fragmented into smaller pieces or the resting actin cytoskeleton could disassemble to monomers and be replaced by a new population of short filaments. The following experiments address the mechanism of this short filament formation.

Readdition of Calcium to Quin-2-loaded Cells Rapidly Dissolved the Actin Filament Bundles in These Cells. As shown in Fig. 9, filopodial forms generated by Quin-2 loading and glass activation of platelets are rapidly converted to forms resembling activated, unchelated platelets when the buffer bathing the cells is replaced with one containing millimolar calcium. Bundles (Fig. 9 *a*) are rapidly reorganized into lamellipodial networks (Fig. 9, *b* and *d*). The effect of added external calcium in the presence of the ionophore A23187 is more drastic. Within seconds, the cytoskeletons of previously chelated cells that contained large actin filament bundles are completely disrupted, leaving a fibrous residue lacking actin filaments (Fig. 9 *d*). This disruption occurs too rapidly to be explained by filaments depolymerizing from their ends. Many actin filaments are also scattered over the surface of the coverslip.

Figure 9. Panel of micrographs demonstrating reversibility of Quin-2-generated filopodial forms by readdition of calcium to the cells. (*a*) Low magnification micrograph of cytoskeletons from Quin-2-preloaded and glass-activated cells. (*b*) Cytoskeletons prepared from cells from the same experiment as in *a* 2 min after the addition of 1 mM calcium to the external medium bathing the cells. (*a*, *b*) The bars are 1 μm. (*c*) Higher magnification micrograph showing the cortex of a cytoskeleton from Quin-2-loaded cells incubated in buffer containing 1 mM calcium as in *b* for 2 min. (*d*) Micrograph showing a representative residue from cells treated as in *a* and then incubated with 1 mM $CaCl_2$ and 20 nM ionophore A23187 for 15 s and then extracted with detergent as in Fig. 1. A fibrous core of unknown composition remains after such treatment. The bulk of cortical actin filaments are removed from cytoskeletons by this treatment (compare with Figs. 1 and 2). Actin filaments that have been dissociated from the core are, however, splayed across the coverslip surface. (*c*, *d*) The bars are 0.1 μm.

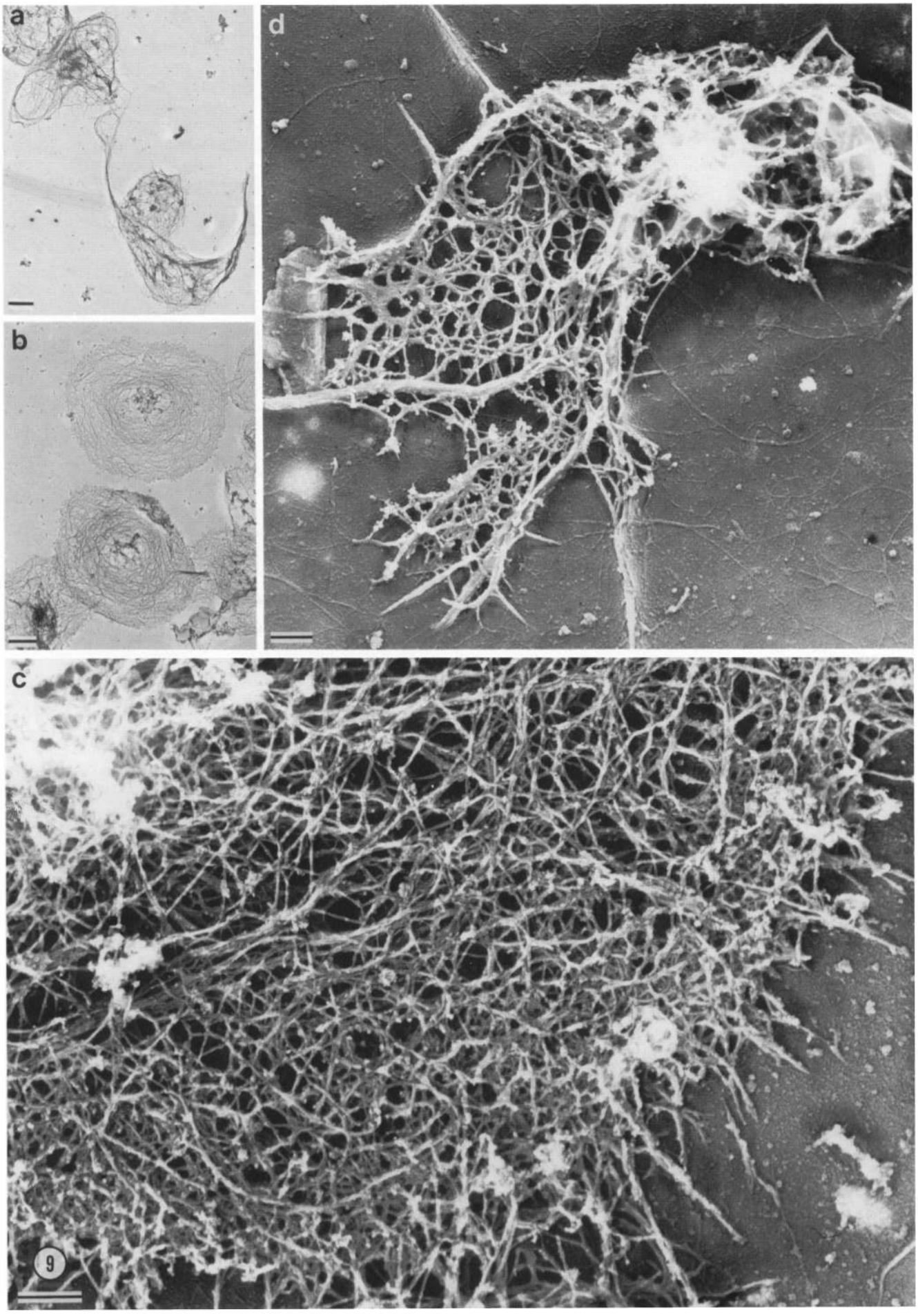
a
b
c
d
9

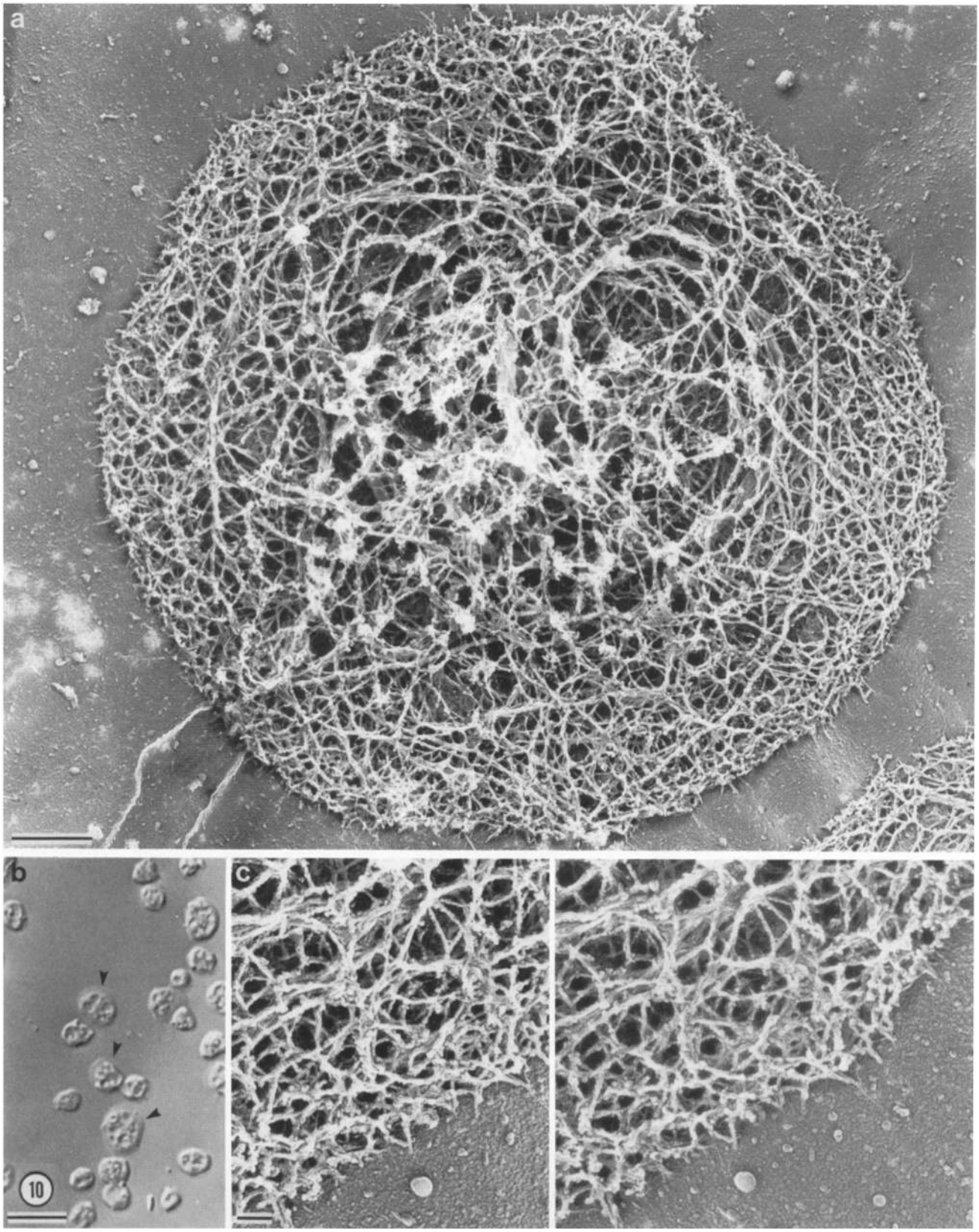

Figure 10. Effect of 2 μM cytochalasin B on the structure of glass-activated platelets and their cytoskeletons. (*a*) Organization of a representative cytoskeleton from a cell treated with cytochalasin B for 5 min before glass activation. Compared with a normal resting cytoskeleton, this cytoskeleton was ~4.5 μm in diameter. This is a 200% increase in the cytoskeletal surface area relative to a cytoskeleton from a resting cell. (*b*) The enlargement of cytochalasin B-treated cells occurs because a circumferential rim of cytoplasm extends beyond the resting cell boundaries after cells are attached to glass by centrifugation. (*c*) This zone of the cytoskeleton is replete with short actin filaments arranged in a three-dimensional network. The bars in *a–c* are 0.5, 5, and 0.1 μm, respectively.

Table III. Effect of Cytochalasin B on the Nucleation Activity in Activated Cytoskeletons

Treatment	Assembly rate (pointed end)	Assembly rate (barbed end*)	Subunits added to pointed ends‡	Subunits added to barbed ends§	Pointed nuclei/platelet	Pointed nuclei/platelet
	$nM\ s^{-1}$	$nM\ s^{-1}$	$\times 10^{10}\ s^{-1}$	$\times 10^{10}\ s^{-1}$		
Resting	0.55 ± 0.15	0.18 ± 0.23	9.95 ± 3.30	2.0	1,980 ± 660	50 ± 20
Activated	0.55 ± 0.18	1.59 ± 0.30	9.95 ± 3.30	39.0	1,980 ± 660	380 ± 50

Resting platelets were incubated with 2 μM cytochalasin B for 5 min, then adhered by centrifugation to 12-mm round glass coverslips coated with polylysine. Cells on the coverslips were exposed to 1 U/ml of thrombin for 30 s in the presence of cytochalasin B and then permeablized with PHEM-Triton buffer. Some coverslips were washed rapidly (1–2 s) through PHEM that did not contain cytochalasin to remove this agent and added to the pyrene-labeled actin assembly system (13). Cytoskeletons from thrombin-treated cells markedly stimulated the rate of actin assembly nucleation activity upon the removal of the cytochalasin B. Cytochalasin B treatment of resting cells did not increase the amount of nucleation activity in resting cytoskeletons. There were 4.2×10^7 platelets per assay. The data are expressed as mean ± SD, $n = 4$.

* The barbed end assembly rate is calculated by subtracting the assembly rate in the presence of 2 μM cytochalasin B from the assembly rate in the absence of cytochalasin B.

‡ Initial pointed end addition rate in 2 μM actin solution was 1.2 subunits s^{-1}.

§ Initial barbed end addition rate in 2 μM actin solution was 18 subunits s^{-1}.

Cytochalasin B Does Not Affect the Amount of Nucleation Activity in Lysates of Activated Cells. In experiments described above, cytochalasin B added to lysates served as a test for the direction (barbed versus pointed) of actin assembly off of nuclei present. In the following experiments, cytochalasin B incubated with intact platelets and later diluted to concentrations in lysates below which it blocks actin assembly permitted the assessment of morphological changes and determination of whether actin nucleation activity appears after platelet activation under a condition in which the bulk of cytoplasmic actin cannot assemble. Fig. 10 shows both the structure of cells centrifuged onto glass coverslips in the presence of cytochalasin B and a representative cytoskeleton from cells permeabilized with detergent in the presence of 2 μM cytochalasin B. As shown in Fig. 10 *b*, cells were unable to change shape markedly in the presence of cytochalasin B, although they were somewhat enlarged and rounded in appearance in the light microscope. Many of the cells had a thin zone of hyaline cytoplasm at their margins (*arrowheads*) not found in untreated resting cells. The origin of morphological changes in these cytochalasin B–treated cells is found by viewing their cytoskeletons in the electron microscope (Fig. 10, *a* and *c*). The cytoskeletal cortex, which corresponds to the hyaline zone, was found to be replete with short, interconnected actin filaments (Fig. 10 *c*).

The generation of nucleation activity after thrombin treatment in the presence of cytochalasin B was demonstrated using the pyrene-labeled actin assembly assay. As shown in Table III, cytoskeletons from thrombin-activated and cytochalasin B–treated cells stimulate the rate of pyrene-actin assembly in vitro fourfold compared with resting cells incubated with cytochalasin B in parallel (to levels comparable to lysates from thrombin-activated cells) when cytochalasin was present while the cells were undergoing activation but washed away before determining nucleation activity. Cytochalasin B treatment of resting cells did not by itself result in nucleation activity. In addition, the rate of actin assembly from the barbed filament ends was near that in cells not exposed to cytochalasin B (compare with Table I). Therefore, these experiments demonstrate that the short filaments found in cytoskeletons from activated cells do not derive from the de novo assembly of actin monomers onto some unspecified barbed end nucleating agent, because cytochalasin B did not inhibit their formation.

To demonstrate that the short actin filaments formed in cells activated in the presence of cytochalasin were calcium dependent, the normal rise in cytosolic calcium was inhibited by loading these cells with Quin-2 and then attaching them to glass by centrifugation in the presence of cytochalasin B. As shown in Fig. 11 *a*, the morphology of these cells was unchanged from that of resting cells. Fig. 11 *b* shows that a cytoskeleton prepared from these cells resembles the structure of the resting platelet cytoskeleton. The cytoskeleton of such cells was discoid and covered with its dense membrane skeleton (compare with Fig. 1 *c* and Figs. 12 and 13 below [12]).

Location of Gelsolin in Resting and Activated Cytoskeletons. The results of the experiments described above implicate calcium-activated actin filament severing as an important step in the remodeling of the resting cytoskeleton into the activated form. Gelsolin accounts for ~0.5% of platelet total protein, yielding a molar ratio of gelsolin to actin of ~1:80, and is an excellent candidate to cause the actin severing observed during platelet activation. Gelsolin was localized in resting and activated cytoskeletons by immunoelectron microscopy. As shown in Fig. 12 *a*, the cytoskeletal gelsolin identified with anti-gelsolin IgG and colloidal-gold particles are found in clusters bound near the membrane skeleton–actin filament interface in thin sections. To determine whether this gelsolin was associated with the ends of actin filaments at this interface or linked to the membrane skeleton, it was localized in mechanically opened cytoskeletons (12) from resting cells (Figs. 12 *b* and 13, *a* and *b*). Micrographs of these preparations demonstrate that: (*a*) gelsolin does not associate with the membrane skeleton per se (Figs. 12 *b* and 13, *a* and *b*); (*b*) gelsolin does associated with the actin filament core lining its surface; (*c*) gold particles are clustered in the core (Figs. 12 *a* and 13 *b*); and (*d*) is on the ends of at least some of the 10-nm filaments knocked out of the cytoskeletons by the mechanical treatment (Figs. 12 *b* and 13 *a*) and is associated with filaments within the filamentous core to the membrane skeleton (Fig. 13). Since the bulk of gelsolin released by detergent treatment of resting cells is gelsolin free (>95%), the large number of gold particles not bound to actin filament ends in these specimens is expected.

As the cytoskeleton changes during spreading, gelsolin also changes in its distribution from the resting condition. As shown in Fig. 13 *d*, gelsolin-reactive gold particles locate in

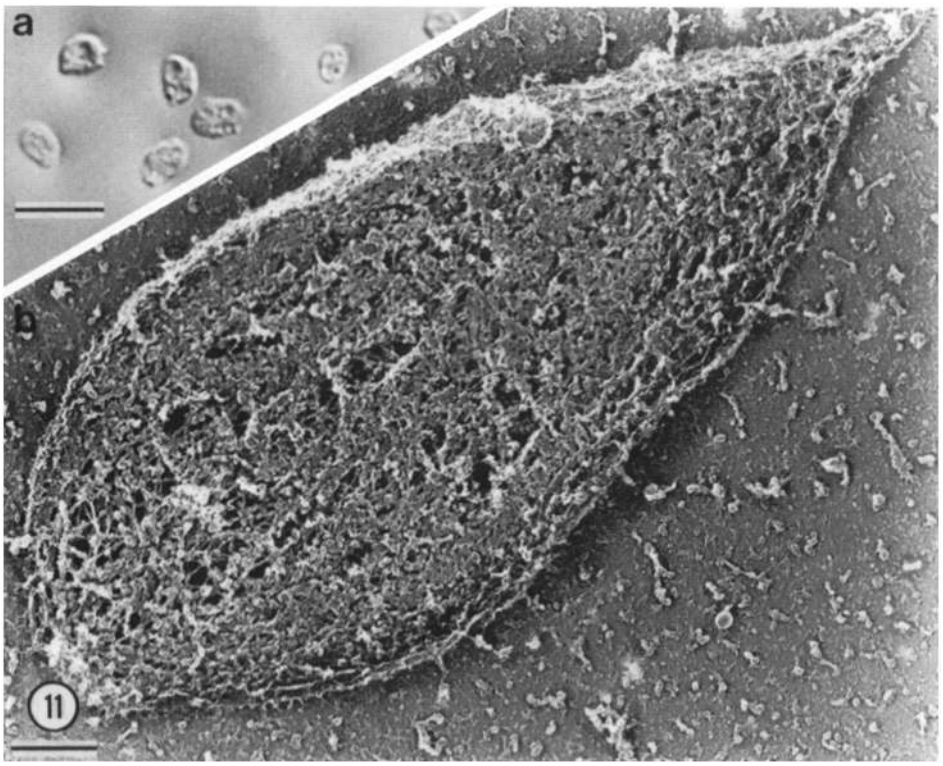

Figure 11. Effect of both cytochalasin B treatment and Quin-2 preloading on the structure of the glass-activated cells. (*a*) DIC light micrograph demonstrating that cells preloaded with Quin-2 and treated with 2 μM cytochalasin B for 5 min before glass activation remain discoid. The bar is 5 μm. (*b*) Representative detergent residue of cells prepared and activated as in *a*. This electron micrograph reveals that little change occurred in the structure of this cytoskeleton relative to cytoskeletons prepared from resting cells. The bar is 0.5 μm.

the lamellipodial zone of the cytoskeleton. Labeling occurred preferentially on one filament end, and less often along filaments. The filament ends decorated with gelsolin-gold were free, were attached to the substratum or pointing upward from it, or intersected the side of another filament to form T-shaped intersections. In marked contrast to resting cells, gold particles in the activated cytoskeleton were not found as large clusters. Filament ends were generally decorated with one to three gold particles. Since only one gelsolin molecule is required to cap the filament end, particle groups of one to three would therefore appear to reflect individual gelsolin molecules. The larger clusters in the resting cytoskeletons would therefore appear to reflect gelsolin clusters.

As shown in Fig. 13 *c*, such rearrangements of gelsolin did not occur in the Quin-2-loaded and activated cells. Gelsolin-reactive gold in these cytoskeletons is more clustered than in the resting cell cytoskeleton. Clusters lie on the sides of actin filaments instead of at their ends.

Discussion

This work confirms many studies showing that the filopodia of activated platelets contain actin filament bundles and demonstrates that these bundles originate within the platelet substance (22, 30, 32). In addition, it provides new details about the structure of actin in lamellae, revealing that it is a tight orthogonal branched network. As expected, neither the filopodial nor lamellipodial actin structures form in platelets activated in the presence of cytochalasin, indicating a requirement for barbed end actin assembly. However, prevention of the usual rise in cytosolic calcium accompanying platelet activation with the permeant calcium chelator Quin-2 inhibited formation of lamellipodial but not filopodial actin structures, indicating that these actin structures are functionally as well as morphologically different (Fig. 14).

Spontaneous actin assembly from monomers in vitro proceeds through a thermodynamically unfavorable nucleation step that limits the initial rate of this polymerization. The presence in platelets of nearly stoichiometric quantities of actin monomer binding proteins such as profilin (28) or β4-thymosin (37, 38) with affinities for actin monomers in the micromolar range would predictably prevent spontaneous nucleation. Lamellipodial and filopodial actin assembly in response to platelet activation therefore requires overcoming

Figure 12. Immunoelectron microscopic localization of gelsolin in the resting platelet cytoskeleton. (*a*) Distribution of 5 nm anti-gelsolin gold in thin sections of Lowicryl-K4M-embedded resting cytoskeletons. The bar is 0.1 μm. Anti-gelsolin colloidal gold is found to label thin sections of cytoskeletons predominantly at the membrane skeleton–actin filament intersection. Gold is generally in clusters of more than five particles. Some of the gold clusters in one region of the cytoskeleton are indicated with arrowheads. Some labeling within the actin core is also observed. (*b*) Location of gelsolin in rapidly frozen resting cytoskeletons. The actin filament core and membrane skeleton of a resting cell were revealed as described previously using mechanical rupture (12). Specimens were fixed and the fixative blocked and labeled with goat anti-gelsolin IgG followed by 8 nm colloidal gold coated with rabbit anti-goat IgG. No labeling was found when primary IgG was omitted, preimmune IgG was used instead of antigelsolin IgG, or gelsolin-adsorbed primary antibody was used (16). Anti-gelsolin gold does not label the membrane skeleton, but does label the actin filament core. Gelsolin gold is also found on the ends of filaments, either those running from the actin filament core to the membrane skeleton (*arrowhead*) or on the ends of filaments knocked out by the rupturing technique (*arrowheads*). The bar is 0.1 μm.

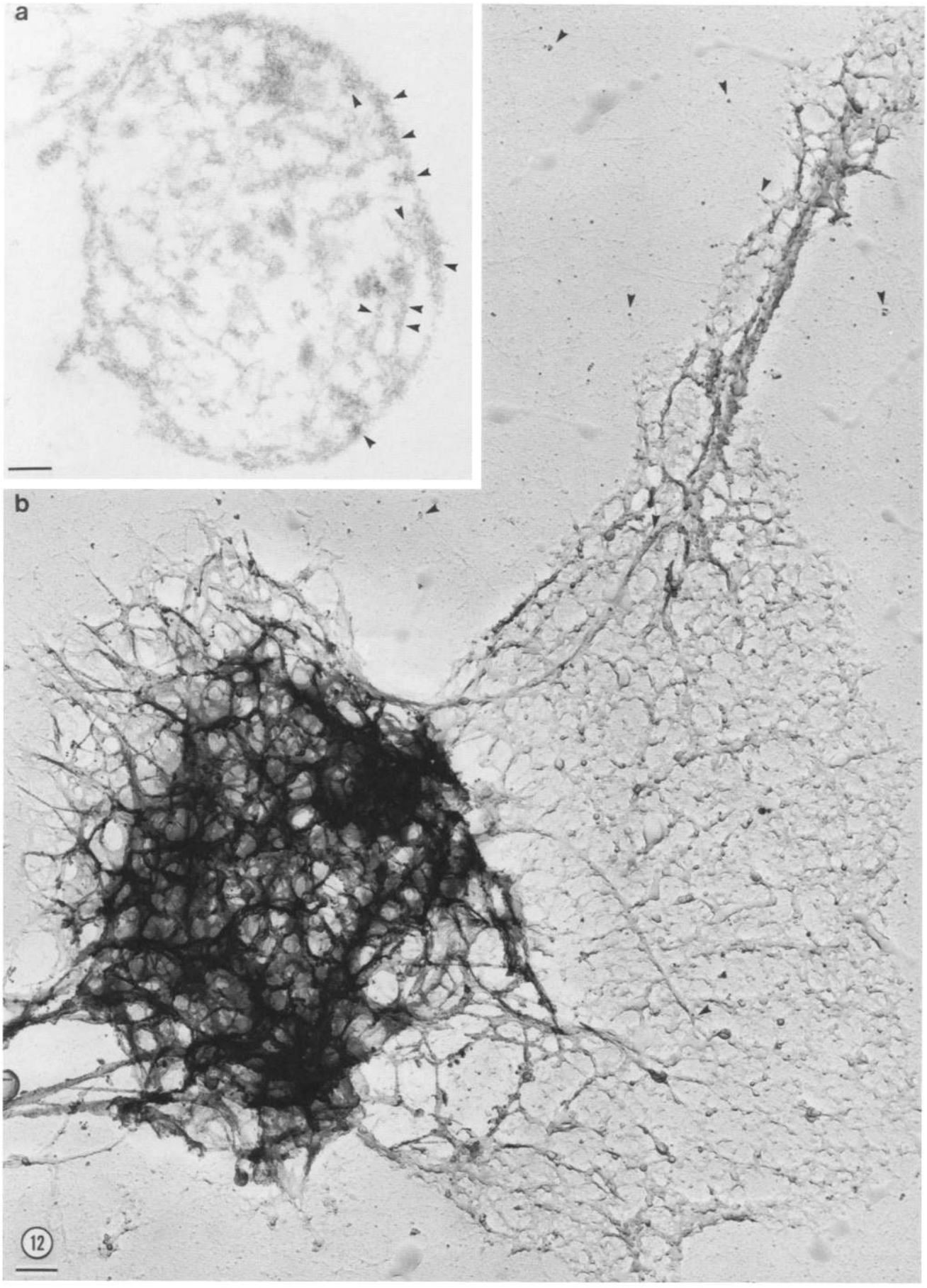
a
b
12

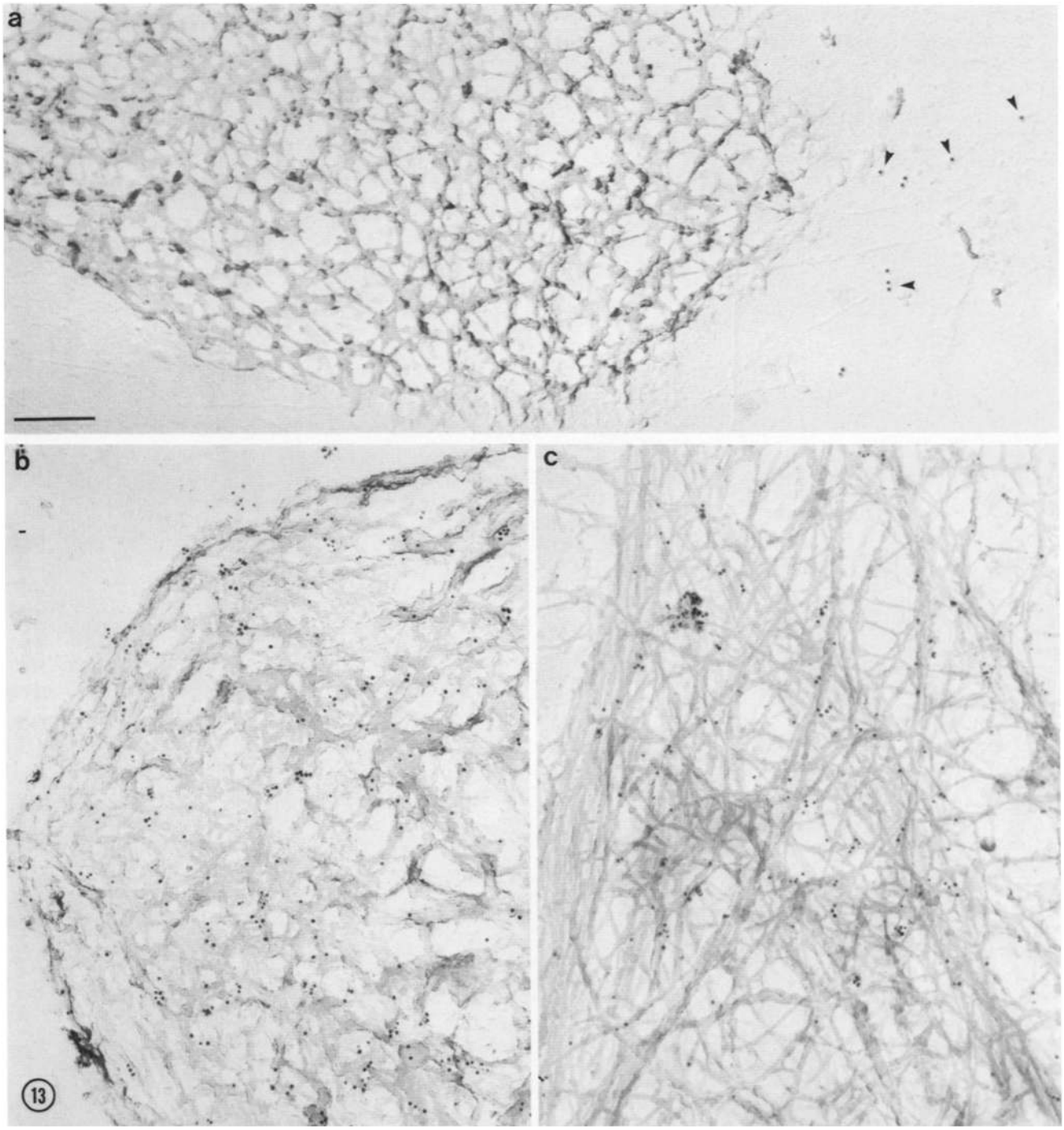

Figure 13. Comparison of the localization of gelsolin between resting and activated cytoskeletons. (*a*, *b*) Electron micrographs demonstrating that gelsolin was not associated with the membrane skeleton (*a*) but is bound along the periphery of the underlying actin filament core (*b*). Membrane skeletons and cores were ruptured by centrifugation. In *a*, some gelsolin can be found on the ends of filaments fragmented from the resting cytoskeleton by the mechanical rupture technique (*arrowheads*). Considerable gelsolin is also shattered across the glass surface in these mechanically disrupted specimens. (*c*) Distribution of gelsolin in glass-activated cytoskeleton from Quin-2-preloaded cell. Anti-gelsolin gold is highly clustered in these cytoskeletons and is found predominantly along the sides of actin filament bundles. (*d*) Distribution of anti-gelsolin 8 nm colloidal gold in the cytoskeleton from an activated cell. One to three gold particles are now found on the ends of short actin filaments. Some of the filament ends having gold particles are indicated with arrowheads. Many gold particles label filament ends that terminate on the sides of other filaments (T-shaped intersections). The bar is 0.1 μm.

the block to spontaneous nucleation at appropriate locations within the platelet. Barbed filament ends are capable of inducing actin polymerization in the presence of profilin (6) and β4-thymosin in vitro (Yin, H. L., unpublished observations) and hence are candidates for the nuclei responsible for initiating actin assembly in activated platelets. Certain actin-associating proteins such as gelsolin, adseverin (scinderin), villin, or Cap Z also promote actin nucleation in vitro, but

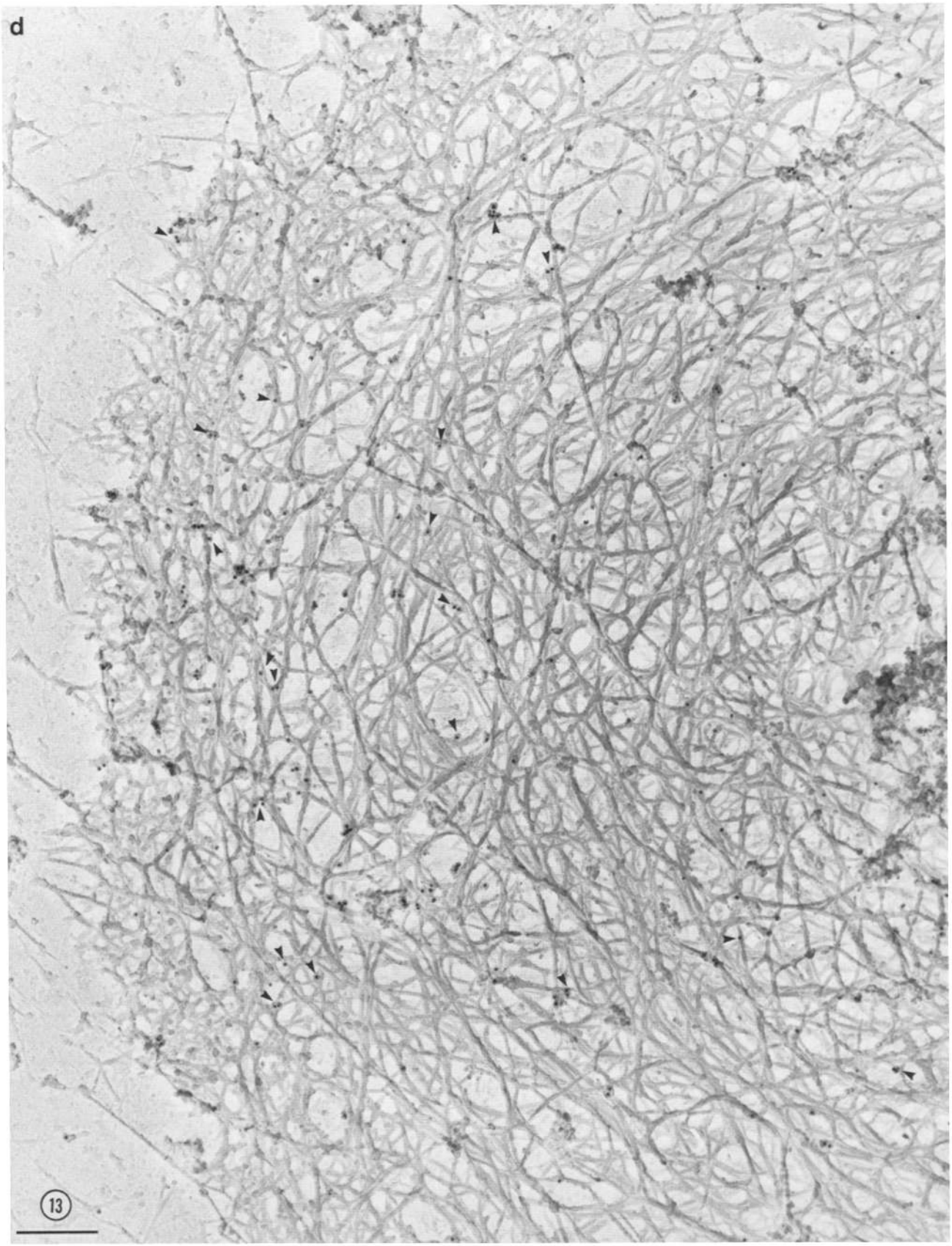

Figure 13.

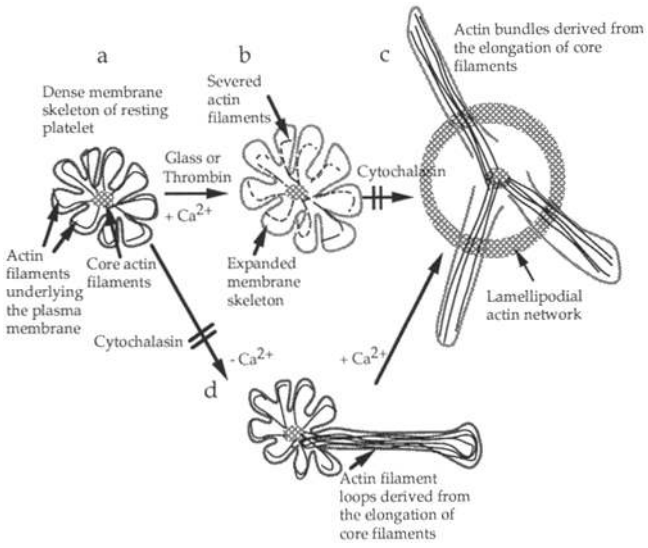

Figure 14. Summary of the control points for actin assembly during platelet shape changes. (*a*) The resting cell. The plasma membrane of the resting human platelet is invested with a dense coat composed of three primary elements: spectrin, ABP, and the attached ends and sides of actin filaments. Actin filaments also form a three-dimensional actin filament core stabilized by ABP molecules. Actin filaments from the core run to the membrane skeleton and end. Barbed actin filament ends are capped in the resting cell. The sides of these filaments are fastened to the membrane by $GPIb_{\alpha\beta}$/IX-ABP complexes. (*b*) Shape changes during activation require the severing of radial actin filaments. This unlocks the membrane skeleton. This step requires an increase in cytosolic calcium concentrations. Calcium-dependent fragmentation of cortical filaments is observed in cells activated in the presence of cytochalasin B. Such cells enlarge and their cytoskeleton is replete with marginal short actin filaments. (*c*) Severing is followed by uncapping of filaments and assembly of actin onto the barbed filament ends. Two zones of assembly are found: filopodia elongating from core actin fibers and lamellipodia growing from the short actin filament templates. (*d*) Shape changes occur also in the absence of calcium transients. Chelated cells elongate and form abnormal filopodia. Actin assembly occurs on the barbed ends of preexisting filaments.

these proteins all block the the barbed end of the formed nucleus and therefore do not lead directly to efficient filament elongation in the presence of actin monomer-binding proteins. These proteins, however, can indirectly elicit nucleation after their dissociation from the barbed ends of filaments by interaction with membrane polyphosphoinositides in vitro. The findings presented here are consistent with such a mechanism operating during platelet activation, although somewhat differently for filopodial and lamellipodial actin assembly. Of the four candidate actin capping proteins, only gelsolin and scinderin have been reported in platelets (27, 46, 51), and of the two, gelsolin is by far the most abundant.

State of Actin in the Resting Cell

Before addressing the origin of the short filaments in the activated cytoskeleton, it is first necessary to understand the state of actin filaments in the resting cell. The kinetic analysis of resting platelet lysates revealed ~2,000 insoluble pointed end nuclei. Since ~40% of total cellular actin is polymerized, there are 780,000 actin subunits in filaments per cell.[2] If the nuclei are filaments of about equal length with capped barbed ends, the average filament length equals 1.1 μm. This is in general agreement with our and others' electron microscopic observations revealing crosslinked 1–3 μm filaments in resting cells (2, 12, 34).

Origin of the Lamellipodial Network

The following discussion summarizes the evidence that calcium-dependent severing of the periphery of the resting platelet's actin skeleton by gelsolin, followed by uncapping of the severed oligomers, leads to formation of the lamellipodial network. For technical convenience in obtaining this evidence, glass-activated platelets were the specimens used for electron microscopy, whereas the nucleation experiments used thrombin-activated platelets. Differences may exist in the mechanics of activation of platelets by thrombin and glass since thrombin is a soluble agonist presented uniformly across the cell surface while glass attachment occurs on only one cell surface. Both stimuli, however, require calcium to change for the effects examined and both lead to similar morphological alterations (31).

The time course for filament rearrangement during activation is too fast to be explained by depolymerization from the pointed ends of preexisting filaments (17). Actin filaments slowly elongate in a pointed direction when assembling in the presence of cytochalasin B, but pointed end growth from a nucleating complex is unlikely given the extent and rate of the structural reorganization during platelet activation. Actin filaments in the resting cell convert in seconds to short filaments by a mechanism unaffected by cytochalasin B. Given the 1.1-μm average starting lengths of the resting fibers, an off rate on the order of two per minute from the pointed filament end (17), and blockage of barbed ends by cytochalasin, monomer dissociation from the pointed end could not shorten the fibers to this extent within 5 min. The results of the nucleation experiments are consistent with >97% of resting filaments being capped on their barbed end in the resting cell.

The interaction of gelsolin with actin is well characterized in resting and thrombin-activated cells. In the resting cell, 95% of the cytoplasmic gelsolin is free, i.e., not complexed to actin (25, 26, 47), as evidenced by the amount of calcium-dependent actin filament severing in such extracts: free gelsolin but not gelsolin-actin complexes sever actin filaments (20). In contrast, gelsolin-actin complexes are more efficient than free gelsolin in promoting nucleation in the pointed direction of actin monomers. Soluble calcium-dependent pointed end nucleation activity was not detectable in resting lysates under the assay conditions used. A small amount of the total gelsolin remains in the detergent insoluble cytoskeleton (25, 26, 44), and ~4% of the total cellular gelsolin associates with the plasma membrane of the resting platelet as assessed by ultrastructural histochemistry (16). In response to thrombin under experimental conditions identical to those used here, gelsolin rapidly binds to actin in an EGTA-resistant complex that has been detected in im-

2. Total actin in a resting platelet is 480 μM. Using the values of Sage and Rink (39) for G and F actin of 280 and 190 μM, respectively, and a platelet volume of 7 fl (33), there are 1.3×10^{-18} mol of F actin per platelet or ($\times$ 6.023×10^{23} molecules/mol) 7.8×10^5 molecules.

munoprecipitates (23, 24, 26). Cytochalasin B–insensitive nuclei equivalent to 5,000 actin filaments were detected in soluble fractions from these activated cells, but only in the presence of calcium, and this activity could be accounted for by the extractable gelsolin in gelsolin-actin complexes.

Calcium at micromolar levels leads to the formation of gelsolin-actin complexes in vitro (45). Thrombin treatment increases cytosolic calcium to near micromolar levels in the absence of external calcium and above micromolar when calcium is a component of the bathing solution (35, 39, 48). Quin-2 loading diminished the actin nucleating activity in lysates of thrombin-treated cells by 60–70%. Loading cells with permeant calcium chelators quenches the cytoplasmic calcium increase in response to agonists (5). Complexing of gelsolin-actin is indicative of filament fragmentation since gelsolin binds more efficiently to actin filaments than monomers (41, 42). Quin-2 loading also prevented the formation of short filaments at the cytoskeletal margins and the filament bundles in Quin-2-loaded and glass-attached cells are disrupted within seconds by the addition of calcium and ionophore. All of these results point to calcium-dependent actin severing by gelsolin as an intermediate step in the formation of lamellar networks.

Some gelsolin is cytoskeletal in the resting platelet. In the resting cytoskeleton, gelsolin clusters at the actin filament–membrane skeletal interface and is found on one end of actin filaments. The clusters may indicate gelsolin bound to PIP (phosphatidylinositol 4-phosphate) or PIP_2 (phosphatidylinositol 4,5-bisphosphate) on the cytoplasmic side of the plasma membrane (21). In cytoskeletons spread on glass, gelsolin aggregates disappear and labeling of a small number of short filament ends becomes predominant. Most filament ends, however, do not label with anti-gelsolin gold, implying that the gelsolin caps have come off these filament ends. This is consistent with the ability of the short filament fragments to nucleate barbed end actin filament growth in vitro. The only known mechanism for dissociating gelsolin as well as most other capping proteins from barbed filament ends is its binding to the membrane polyphosphoinositides, phosphatidylinositol monophosphate and phosphatidylinositol 4,5-bisphosphate (18, 19). Since gelsolin traffics to the membrane with activation, these are prime candidates for the uncapping function (16). Uncapping of filaments by changes in polyphosphoinositide concentration or physical state could clearly be localized to these few sites where the ends interface the membrane, accounting for the failure in some systems to correlate changes in the bulk polyphosphoinositide level with gelsolin-actin complex during cell activation (43).

Formation of Filopodial Bundles

Platelets loaded with Quin-2 did not extend lamellipodial networks; instead, cells protruded unusual spikes. Spikes elongate from the barbed ends of preexisting filaments which uncap as evidenced by loss of immunoreactive gelsolin from barbed ends of preexisting core filaments, growth of added monomeric actin onto the barbed ends of filopodial actin filaments in extracted cytoskeletons, and the appearance of some cytochalasin B–sensitive actin nucleation activity in cytoskeletons of Quin-2-loaded thrombin-activated platelets. Uncapping without fragmentation supplies one-fourth the number of nuclei and leads to abnormal shape changes. Monomer activation would lead to elongation. Fragmentation, therefore, amplifies activation by increasing the total number of nucleation sites. Elongation limited to preexisting filaments also distorts cells. Since the ends of the preexisting core filaments are in contact with and run parallel to the plasma membrane, filament elongation occurs preferentially along the cytoplasmic membrane surface. Some fibers may also elongate perpendicular to the plasma membrane and may provide the mechanical force for localized outpockets of membrane in these cells.

The agents that cap barbed actin filament ends in the resting cell are unknown, but gelsolin is a likely candidate. Sufficient gelsolin complexes actin in the resting cell to cap this small number of barbed filament ends (23, 24, 26), and at least some of these fibers have immunologically detectable gelsolin on their ends in the resting cytoskeleton. Whether additional proteins laterally aggregate the fibers into the filopodial bundles is unknown but likely (31). The fragmentation of actin filaments could also disrupt the membrane skeleton at distinct points, which could create holes through which filaments elongate.

The Role of the Membrane Skeleton in Activation

Resting platelets have a smooth surface interrupted only by invaginations of their plasma membrane. This unusual internal packaging of redundant plasma membrane may increase the stability of a surface at risk from the shearing forces of circulation. The maintenance of membrane in this conformation may require the resting cell to have an elaborate membrane skeleton, both to stabilize the plasma membrane and to anchor it to a three-dimensional actin filament core.

The membrane skeleton of the resting platelets is a spectrin-based shell (4, 10–12) directly attached to the ends of actin filaments and indirectly attached to these same filaments by ABP molecules connecting $GPIb_{\alpha\beta}$/IX complexes. The importance of ABP-$GPIb_{\alpha\beta}$/IX-actin filament connections to the structure of the membrane skeleton was demonstrated previously when perturbations that removed the underlying actin filaments, and hence the $GPIb_{\alpha\beta}$/IX complexes, loosened and simplified the structure of the membrane skeleton. In the resting cell, the spectrin-based lattice is therefore held in a compacted state by underlying actin filaments-ABP-$GPIb_{\alpha\beta}$/IX connections. Severing by gelsolin of the filaments underlying the plasma membrane between ABP-$GPIb_{\alpha\beta}$/IX links is an effective mechanism to detach the membrane skeleton from most of its actin filament connections. The advantages of severing are twofold. First, the fragments are subsequently uncapped and used as nucleation sites for filament assembly. Second, the short filaments remain membrane associated via the ABP and spectrin connections, thereby providing spatial information for new assembly. The total filament number per resting cell is comparable to that of spectrin tetramers in the platelet membrane skeleton. This correlation suggests that the end of each filament might be fastened directly to the membrane skeleton by spectrin. ABP, on the other hand, is considerably more abundant as there are six molecules of ABP for each cytosolic 0.6-μm filament. Filaments could be linked every 100 nm or so to $GPIb_{\alpha\beta}$/IX complexes in the membrane using ABP molecules. This high ratio of ABP to actin ex-

plains the stable association of fragmented filaments with the cytoskeletons of activated cells.

I thank Dr. Thomas P. Stossel for his supportive environment, wonderful ideas, and helpful criticism, Ms. Darlene M. Jackson for her editorial and secretarial skills, and Ms. Michelle DeSisto, Ms. Andrea Franciso, and Ms. Rebecca Winokur for technical assistance.

This work was supported by United States Public Health Services grant HL-47874 and by a grant from the Edwin S. Webster Foundation.

Received for publication 19 December 1991 and in revised form 14 April 1992.

References

1. Allen, R., L. Zacharski, S. Widirstky, R. Rosenstein, L. Zaitlin, and D. Burgess. 1979. Transformation and motility of human platelets. *J. Cell Biol.* 83:126–142.
2. Boyles, J., J. E. B. Fox, D. R. Phillips, and P. E. Stenberg. 1985. Organization of the cytoskeleton in resting, discoid platelets: Preservation of actin filaments by a modified fixation that prevents osmium damage. *J. Cell Biol.* 101:1463–1472.
3. Casella, J. F., M. D. Flanagan, and S. Lin. 1981. Cytochalasin D inhibits actin polymerization and induces depolymerization of actin filaments formed during platelet shape change. *Nature (Lond.).* 293:302–305.
4. Davies, G. E., and C. M. Cohen. 1985. Platelets contain proteins immunologically related to red cell spectrin and protein 4.1. *Blood.* 65:52–59.
5. Davies, T., D. Drotts, G. Weil, and E. Simons. 1989. Cytoplasmic Ca^{2+} is necessary for thrombin-induced platelet activation. *J. Biol. Chem.* 264: 19600–19606.
6. DiNubile, M. J., and F. S. Southwick. 1985. Effects of macrophage profilin on actin in the presence and absence of acumentin and gelsolin. *J. Biol. Chem.* 260:7402–7409.
7. Di Virgilio, F., B. Meyer, S. Greenberg, and S. Silverstein. 1988. Fc receptor-mediated phagocytosis occurs in macrophages at exceedingly low cytosolic Ca^{2+} levels. *J. Cell Biol.* 106:657–666.
8. Fox, J. E. B., and D. R. Phillips. 1981. Inhibition of actin polymerization in blood platelets by cytochalasins. *Nature (Lond.).* 292:650–652.
9. Fox, J., D. Goll, C. Reynolds, and D. Phillips. 1985. Identification of two proteins (actin-binding protein and P235) that are hydrolyzed by endogenous Ca^{2+}-dependent protease during platelet aggregation. *J. Biol. Chem.* 260:1060–1066.
10. Fox, J., C. Reynolds, J. Morrow, and D. Phillips. 1987. Spectrin is associated with membrane-bound actin filaments in platelets and is hydrolyzed by the Ca^{2+}-dependent protease during platelet activation. *Blood.* 69:537–545.
11. Fox, J., J. Boyles, M. Berndt, P. Steffen, and L. Anderson. 1988. Identification of a membrane skeleton in platelets. *J. Cell Biol.* 106: 1525–1538.
12. Hartwig, J., and M. DeSisto. 1991. The cytoskeleton of the resting human blood platelet. Structure of the membrane skeleton and its attachment to actin filaments. *J. Cell Biol.* 112:407–425.
13. Hartwig, J., and P. Janmey. 1989. Stimulation of a calcium-dependent actin nucleation activity by phorbol 12-myristate 13-acetate in rabbit macrophage cytoskeletons. *Biochim. Biophys. Acta.* 1010:64–71.
14. Hartwig, J., and P. Shevlin. 1986. The architecture of actin filaments and the ultrastructural location of actin-binding protein in the periphery of lung macrophages. *J. Cell Biol.* 103:1007–1020.
15. Hartwig, J., K. Chambers, K. Hopica, and D. Kwiatkowski. 1989. Association of profilin with filament-free regions of human leukocyte and platelet membranes and reversible membrane-binding during platelet activation. *J. Cell Biol.* 109:1571–1579.
16. Hartwig, J., K. Chambers, and T. Stossel. 1989. Association of gelsolin with actin filaments and cell membranes of macrophages and platelets. *J. Cell Biol.* 109:467–479.
17. Janmey, P. A., and T. P. Stossel. 1986. Kinetics of actin monomer exchange at the slow growing ends of actin filaments and their relation to the elongation of filaments shortened by gelsolin. *J. Muscle Res. Cell Motil.* 7:446–454.
18. Janmey, P., and T. Stossel. 1987. Modulation of gelsolin function by phosphatidylinositol 4,5-bisphosphate. *Nature (Lond.).* 325:362–364.
19. Janmey, P., and T. Stossel. 1989. Gelsolin-polyphosphoinositide interaction. Full expression of gelsolin-inhibiting function by polyphosphoinositides in vesicular form and inactivation by dilution, aggregation, or masking of the inositol head group. *J. Biol. Chem.* 264:4825–4831.
20. Janmey, P. A., C. Chaponnier, S. E. Lind, K. S. Zaner, T. P. Stossel, and H. L. Yin. 1985. Interactions of gelsolin and gelsolin actin complexes with actin: effects of calcium on actin nucleation, filament severing and end blocking. *Biochemistry.* 24:3714–3723.
21. Janmey, P. A., K. Iida, H. L. Yin, and T. P. Stossel. 1987. Polyphosphoinositide micelles and polyphosphoinositide-containing vesicles dissociate endogenous gelsolin-actin complexes and promote actin assembly from the fast-growing end of actin filaments blocked by gelsolin. *J. Biol. Chem.* 262:12228–12236.
22. Karlsson, R., I. Lassing, A.-S. Hoglund, and U. Lindberg. 1984. The organization of microfilaments in spreading platelets: a comparison with fibroblasts and glial cells. *J. Cell. Physiol.* 121:96–113.
23. Kurth, M., and J. Bryan. 1984. Platelet activation induces the formation of a stable gelsolin-actin complex from monomeric gelsolin. *J. Biol. Chem.* 259:7473–7479.
24. Kurth, M. C., L. L. Wang, J. Dingus, and J. Bryan. 1983. Purification and characterization of a gelsolin-actin complex from human platelets. *J. Biol. Chem.* 258:10895–10903.
25. Lind, S., H. L. Lin, and T. P. Stossel. 1982. Human platelets contain gelsolin, a regulator of actin filament length. *J. Clin Invest.* 69:1384–1387.
26. Lind, S. E., P. A. Janmey, C. Chaponnier, T. Herbert, and T. P. Stossel. 1987. Reversible binding of actin to gelsolin and profilin in human platelet extracts. *J. Cell Biol.* 105:833–842.
27. Maekawa, S., and H. Sakai. 1990. Inhibition of actin regulatory activity of the 74-kDa protein from bovine adrenal medulla (Adseverin) by some phospholipids. *J. Biol. Chem.* 265:10940–10942.
28. Markey, F., U. Lindberg, and L. Eriksson. 1978. Human platelets contain profilin, a potential regulator of actin polymerizability. *FEBS Letters.* 88:75–79.
29. Markey, F., T. Persson, and U. Lindberg. 1981. Characterization of platelet extracts before and after stimulation with respect to the possible role of profilactin as microfilament precursor. *Cell.* 23:145–153.
30. Nachmias, V. 1980. Cytoskeleton of human platelets at rest and after spreading. *J. Cell Biol.* 86:795–802.
31. Nachmias, V. T., and K. Yoshida. 1988. The cytoskeleton of the blood platelet: a dynamic structure. *Adv. Cell Biol.* 2:181–211.
32. Nachmias, V., J. Sullender, J. Fallon, and A. Asch. 1979. Observations on the "cytoskeleton" of human platelets. *Thrombo. Haemostasis.* 42:1661–1666.
33. Nachmias, V., K. Yoshida, and M. Glennon. 1987. Lowering pHi dissociated myosin phosphorylation from shape change and myosin association with the cytoskeleton. *J. Cell Biol.* 105:1761–1769.
34. Nakata, T., and N. Hirokawa. 1987. Cytoskeletal reorganization in human platelets after stimulation revealed by the quick-freeze deep-etch technique. *J. Cell Biol.* 105:1771–1780.
35. Oda, A., J. Daley, J. Kang, M. Smith, J. Ware, and E. Salzman. 1991. Quasi-simultaneous measurement of ionized calcium and α-granule release in individual platelets. *Am. J. Physiol.* 260:C242–C248.
36. Okita, L., D. Pidard, P. Newman, R. Montgomery, and T. Kunicki. 1985. On the association of glycoprotein Ib and actin-binding protein in human platelets. *J. Cell Biol.* 100:317–321.
37. Safer, D., R. Golla, and V. Nachmias. 1990. Isolation of a 5-kilodalton actin-sequestering peptide from human blood platelets. *Proc. Natl. Acad. Sci. USA* 87:2536–2539.
38. Safer, D., M. Elzinga, and V. T. Nachmias. 1991. Thymosin B4 and Fx, an actin-sequestering peptide, are indistinguishable. *J. Biol. Chem.* 266:4029–4032.
39. Sage, S., and T. Rink. 1987. The kinetics of changes in intracellular calcium concentration in fura-2-loaded human platelets. *J. Biol. Chem.* 262: 16364–16369.
40. Schliwa, M., J. van Blerkom, and K. Porter. 1981. Stabilization of the cytoplasmic ground substance in detergent-opened cells and a structural and biochemical analysis of its composition. *Proc. Natl. Acad. Sci. USA* 80:5417–5420.
41. Schoepper, B., and A. Wegner. 1991. Rate constants and equilibrium constants for binding of actin to the 1:1 gelsolin-actin complex. *FEBS Letters.* 202:1127–1131.
42. Selve, N., and A. Wegner. 1986. Rate constants and equilibrium constants for binding of the gelsolin-actin complex to the barbed ends of actin filaments in the presence and absence of calcium. *Eur. J. Biochem.* 160: 379–387.
43. Shariff, A., and E. Luna. 1992. Diacylglycerol-stimulated formation of actin nucleation sites at plasma membranes. *Science (Wash. DC).* 256: 245–247.
44. Slot, J., and H. Geuze. 1985. A new method of preparing gold probes for multiple-labeling cytochemistry. *Eur. J. Cell Biol.* 38:87–93.
45. Stossel, T. 1989. From signal to pseudopod. How cells control cytoplasmic actin assembly. *J. Biol. Chem.* 264:18261–18264.
46. Tchakarov, L., M.-L. Vitale, M. Jeyaprogasan, A. Rodriguez Del Castillo, and J.-M. Trifaro. 1990. Expression of scinderin, an actin filament-severing protein, in different tissues. *FEBS. Letters.* 268:209–212.
47. Wang, L. L., and J. Bryan. 1981. Isolation of calcium-dependent platelet proteins that interact with actin. *Cell.* 25:637–649.
48. Ware, J., P. Johnson, M. Smith, and E. Salzman. 1986. Effect of common agonists on cytoplasmic ionized calcium concentration in platelets. *J. Clin. Invest.* 77:878–886.
49. White, J. 1984. Arrangements of actin filaments in the cytoskeleton of human platelets. *Am. J. Pathol.* 117:207–217.
50. White, J., G. Escolar, and E. Leistikow. 1989. GPIIb-IIIa receptor mobility within membranes of surface and suspension activated platelets does not depend on assembly and contraction of cytoplasmic actin. *Clin. Res.* 37:603a (Abstr.)
51. Yin, H. L. 1988. Gelsolin: a calcium- and polyphosphoinositide-regulated actin-modulating protein. *BioEssays.* 7:176–179.
52. Zucker-Franklin, D. 1970. The ultrastructure of megakaryocytes and platelets. *In* Regulation of Hematopoiesis. A. Gordon, editor. Appleton-Century Crofts, New York. 1553–1586.